Journal of Statistical Physics, Vol. 119, Nos. 3/4, May 2005 (© 2005)
DOI: 10.1007/s10955-004-3247-7

Anisotropy Effects in Nucleation for Conservative Dynamics

F.R. Nardi[1], E. Olivieri[2], and E. Scoppola[3]

Received August 5, 2004; accepted December 30, 2004

We analyze metastability and nucleation in the context of a local version of the Kawasaki dynamics for the two-dimensional *anisotropic* Ising lattice gas at very low temperature. Let $\Lambda \subset \mathbb{Z}^2$ be a sufficiently large finite box. Particles perform simple exclusion on Λ, but when they occupy neighboring sites they feel a binding energy $-U_1 < 0$ in the horizontal direction and $-U_2 < 0$ in the vertical direction; we assume $U_1 \geqslant U_2$. Along each bond touching the boundary of Λ from the outside, particles are created with rate $\rho = e^{-\Delta\beta}$ and are annihilated with rate 1, where β is the inverse temperature and $\Delta > 0$ is an activity parameter. Thus, the boundary of Λ plays the role of an infinite gas reservoir with density ρ. We take $\Delta \in (U_1, U_1 + U_2)$ where the totally empty (full) configuration can be naturally associated to metastability (stability). We investigate how the transition from empty to full takes place under the dynamics. In particular, we identify the size and some characteristics of the shape of the *critical droplet* and the time of its creation in the limit as $\beta \to \infty$. We observe very different behavior in the weakly or strongly anisotropic case. In both case we find that Wulff shape is not relevant for the nucleation pattern.

KEY WORDS: Lattice gas; Kawasaki dynamics; metastability; critical droplet; large deviations.

1. INTRODUCTION

In this paper, we study the metastable behavior of the two-dimensional anisotropic Ising lattice gas subject to Kawasaki dynamics. We consider

[1]Dipartimento di Matematica, Università di Roma La Sapienza, Piazzale Aldo Moro 2, 00100 Rome, Italy; e-mail: nardi@mat.uniroma2.it
[2]Dipartimento di Matematica, Università di Roma Tor Vergata, Via della Ricerca Scientifica, 00133 Rome, Italy; e-mail: olivieri@mat.uniroma2.it
[3]Dipartimento di Matematica, Università di Roma Tre, Largo S. Leonardo Murialdo 1, 00146 Rome, Italy and Istituto Nazionale di Fisica della Materia, Unità di Roma 1, Rome, Italy; e-mail: scoppola@mat.uniroma3.it

the "local version" of the model, where particles live and evolve in a conservative way on a finite box Λ and are created resp. annihilated at the boundary of this box in a way that reflects an infinite gas reservoir. In this way the number of particles is not globally conserved and the equilibrium will be described by means of a grand-canonical Gibbs measure with a chemical potential which is related to the rate of creation of particles at the boundary.

We introduce a stochastic dynamics given by a discrete time Metropolis algorithm (we refer to (1.9), see also ref. 15). In particular the detailed balance condition is satisfied with respect to the Gibbs grand-canonical measure corresponding to the Ising Hamiltonian (see (1.2)). We call U_1, U_2 the binding energy between two nearest–neighbor particles in the horizontal and vertical direction, respectively. Without loss of generality we always suppose $U_1 \geqslant U_2$. We consider the asymptotic regime corresponding to fixed volume and chemical potential in the limit of large inverse temperature β. The above setup gives rise to a reversible Freidlin Wentzell Markov chain (see ref. 15).

Our results generalize part of those obtained by den Hollander *et al.*[8], where, in particular, the same model was considered with isotropic interaction ($U_1 = U_2$). In ref. 7, the three-dimensional isotropic case was considered. In this paper, we consider only the two-dimensional case and we choose the parameters of the interaction so that the empty and full configurations are naturally associated to the metastable and stable states. We identify the size and shape of the critical droplet and the time of its creation in the limit of low temperature. Our results are comparable with but less complete than those obtained by Kotecký and Olivieri[9] for the anisotropic Ising model subject to Glauber dynamics. Kawasaki dynamics has its own characteristics, which need to be handled in the description of the nucleation. Particle conservation in the interior of the box represents a serious obstacle in controlling the growing and the shrinking of droplets.

It will turn out that a complete description of the metastable behavior, as given in ref. 9 for Glauber dynamics, is much more complicated for Kawasaki dynamics. The isotropic case is simpler but still quite complicated. In this context in ref. 6, a description of the tube of typical trajectories is given. In the present paper we do not obtain such a complete description. We remark that in many previous papers[1,4,5,7,9,10,12] the asymptotic of the tunnelling time and the tube of typical trajectories realizing the transition were treated simultaneously by exploiting a detailed control of the landscape of energy in connection with the paths allowed by the dynamics.

In this paper, following the strategy proposed in ref. 11, we are able to determine the asymptotic behavior in probability, for large β, of the

transition time between the empty and full configuration. Indeed using ref. 11 the control of the transition time can be obtained on the basis of relatively weak hypotheses: the knowledge of the global saddles between the metastable and the stable state together with the absence of too "deep wells".

We also have some partial information on the typical trajectories realizing the transition between metastability and stability. Indeed we discuss in detail the critical droplet representing the "gate" to the stable state.

Let us now discuss the motivations and the specific features of our model by outlining the main results.

In the Freidlin Wentzell regime it is natural to call Wulff shape the one minimizing the energy of a droplet at fixed volume. Indeed at low temperature only the energy is relevant not entropy. In our case this is a rectangle with horizontal and vertical sides proportional, respectively, to the corresponding coupling constants U_1 and U_2 (see ref. 9).

The main question that is natural to address concerns the relevance of Wulff shape in the nucleation pattern. It turns out that particles can move along the border of a droplet more rapidly than they can arrive from the boundary of the container by inducing the growth of the droplet.

One could be tempted to conjecture that this displacement along the border of the growing droplet should be able to establish the equilibrium shape at fixed volume namely, the Wulff shape. However, a careful comparison between time scales of contraction, growth and of different types of movements on the border, shows that the above conjecture is false.

The critical configurations are different and more complicated than the ones for Ising spins under Glauber dynamics (even in the anisotropic case).

We observe very different behavior of our model for weak or strong anisotropy, corresponding, roughly speaking, to U_1 smaller or larger than $2U_2$ (see (1.49) for more details).

For weak anisotropy a rigorous result that we are able to prove is that the critical droplet is close to the Wulff shape (with a highly degenerate and complicated microscopic structure) whereas we have strong indications that during the other stages of nucleation, namely both in the subcritical and supercritical part, the shape of the growing droplet is not Wulff. Actually large supercritical droplets tend to have a squared shape contrary to what happens for the non-conservative Glauber dynamics.

For strong anisotropy the critical droplet is not Wulff and the Wulff shape is crossed during the supercritical growth.

In both cases the Wulff shape is not relevant in the nucleation pattern, similarly to what came out in the Glauber case (see refs. 9 and 10).

In order to predict, at least at the heuristic level the nucleation pattern, we have to analyze the various mechanisms of modification of a rectangular droplet. We restrict ourselves to rectangles since, as is easy to

verify, every cluster is transformed with high probability into a rectangle in a relatively short time. Suppose we are given a rectangle with horizontal side l_1 and vertical side l_2. Suppose that the occupied sites are precisely the ones contained inside the rectangle. The typical mechanisms to add or remove a row or a column from a rectangle are similar to the corresponding mechanisms occurring in non-conservative Glauber dynamics; but now, in our locally conservative dynamics, an important role is played by an additional mechanism involving the displacement of particles along the border of the rectangle. It consists either

(I) of the loss of a row with the simultaneous gain of a column: $(l_1, l_2) \to (l_1 + 1, l_2 - 1)$; or

(II) of the loss of a column with the simultaneous gain of a row: $(l_1, l_2) \to (l_1 - 1, l_2 + 1)$

(I) and (II) can also involve, beyond locally conservative moves, creation or annihilation of particles at the boundary of the container to get the final rectangle.

It is reasonable to expect that the mechanism (I) is preferred when l_2 is sufficiently large in terms of l_1 whereas (II) is preferred in the opposite case. The characteristic shape corresponding to a balance between the two mechanisms gives rise to a sort of equilibrium that corresponds to a minimum of the energy at fixed perimeter and that is not Wulff.

For sufficiently large rectangles, this balance takes place when $l_1 - l_2 \sim \bar{l}$ with $\bar{l}$ a suitable constant depending on the coupling constants of the model (see (1.37)). A rectangle with such a shape is called *standard* (see point 6 in Section 1.3 for a precise definition).

As discussed heuristically in Section 2.2, for weak anisotropy, we expect that, after an initial stage which we are going to describe in a while, the nucleation pattern consists of a growing sequence of standard rectangles. The critical droplet belongs to this sequence, and it happens that it is, at the same time, standard and Wulff but this has to be considered as an accident. Clearly, large supercritical standard rectangles are almost squared. This behavior is very different with respect to the one of non-conservative dynamics where, for any degree of anisotropy, the supercritical growth is highly anisotropic (see ref. 9).

Quite surprisingly, in the early stage of nucleation we have a growth along *domino* shape with $l_1 \sim 2l_2$ independently on the parameters of the interaction (see point 6 in Section 1.3).

In the case of strong anisotropy $U_1 > 2U_2$ we develop the above heuristic discussion coming to the conclusion that the growth follows the

domino shape up to the critical droplet which therefore is not Wulff; indeed in this case the ratio between the side lengths of a Wulff rectangle is larger than 2, the value corresponding to domino shape. Let $\hat{l}_1, \hat{l}_2$ be the horizontal and vertical sides, respectively, of the critical droplet. In this strongly anisotropic case the supercritical growth follows a sequence of rectangles with $l_2 = \hat{l}_2$ and $l_1 = \hat{l}_1 + m$, with $m = 1, 2, \ldots$ up to $l_1 = L$ the side of the container. During this epoch, the nucleation pattern crosses the Wulff shape. Finally, after the formation of a strip $\hat{l}_2 \times L$ the system starts growing in the vertical direction up to the full configuration.

This behavior in the strongly anisotropic case is more similar to what happens in the corresponding Glauber case for any degree of anisotropy.

In the remaining part of this section we give definitions and the main theorem.

In Section 2 we give a heuristic discussion of the problem from a statical and from a dynamical point of view. Section 3 contains the proof of the theorems.

1.1. Definition of the Model

Let $\Lambda \subset \mathbb{Z}^2$ be a finite box centered at the origin that will be chosen large enough. Let

$$\partial^- \Lambda = \{x \in \Lambda: \ \exists\, y \notin \Lambda: \ |y - x| = 1\} \tag{1.1}$$

be the interior boundary of Λ and let $\Lambda_0 = \Lambda \setminus \partial^- \Lambda$ be the interior of Λ. With each $x \in \Lambda$ we associate an occupation variable $\eta(x)$, assuming values 0 or 1. A lattice configuration is denoted by $\eta \in \mathcal{X} = \{0, 1\}^\Lambda$. We often identify η with its support, i.e. the set of occupied sites in η.

Each configuration $\eta \in \mathcal{X}$ has an energy given by the following Hamiltonian:

$$H(\eta) = -U_1 \sum_{(x,y) \in \Lambda^*_{0,h}} \eta(x)\eta(y) - U_2 \sum_{(x,y) \in \Lambda^*_{0,v}} \eta(x)\eta(y) + \Delta \sum_{x \in \Lambda} \eta(x), \tag{1.2}$$

where $\Lambda^*_{0,h}$ (resp. $\Lambda^*_{0,v}$) is the set of the horizontal (vertical) unoriented bonds joining n.n. points in Λ_0. Thus the interaction is acting only inside Λ_0; the binding energy associated to a horizontal (vertical) bond is $-U_1 < 0$ ($-U_2 < 0$). We can suppose without loss of generality that $U_1 \geqslant U_2$. (Note that $H - \Delta \sum_{x \in \partial^- \Lambda} \eta(x)$ can be viewed as the Hamiltonian, in lattice gas variables, for an Ising system enclosed in Λ_0, with 0 boundary conditions.)

The grand-canonical Gibbs measure associated with H is

$$\mu(\eta) = \frac{e^{-\beta H(\eta)}}{Z}, \quad \eta \in \mathcal{X}, \tag{1.3}$$

where

$$Z = \sum_{\eta \in \mathcal{X}} e^{-\beta H(\eta)}. \tag{1.4}$$

1.2. Local Kawasaki Dynamics

We next define Kawasaki dynamics on Λ, with a boundary condition that mimicks the effect of an infinite gas reservoir outside Λ with density $\rho = e^{-\Delta\beta}$. Let $b = (x \to y)$ be an oriented bond, i.e. an *ordered* pair of nearest-neighbor sites, and define

$$\begin{aligned} \partial^* \Lambda^{\text{out}} &= \{b = (x \to y) \colon\ x \in \partial^- \Lambda,\ y \notin \Lambda\}, \\ \partial^* \Lambda^{\text{in}} &= \{b = (x \to y) \colon\ x \notin \Lambda,\ y \in \partial^- \Lambda\}, \\ \Lambda^{*,\text{orie}} &= \{b = (x \to y) \colon\ x, y \in \Lambda\}, \end{aligned} \tag{1.5}$$

and put $\bar{\Lambda}^{*,\text{orie}} = \partial^* \Lambda^{\text{out}} \cup \partial^* \Lambda^{\text{in}} \cup \Lambda^{*,\text{orie}}$. Two configurations $\eta, \eta' \in \mathcal{X}$ with $\eta \neq \eta'$ are said to be *communicating states* if there exists a bond $b \in \bar{\Lambda}^{*,\text{orie}}$ such that $\eta' = T_b \eta$, where $T_b \eta$ is the configuration obtained from η as follows:

for $b = (x \to y) \in \Lambda^{*,\text{orie}}$, $T_b \eta$ denotes the configuration obtained from η by interchanging particles along b:

$$T_b \eta(z) = \begin{cases} \eta(z) & \text{if } z \neq x, y, \\ \eta(x) & \text{if } z = y, \\ \eta(y) & \text{if } z = x \end{cases} \tag{1.6}$$

for $b = (x \to y) \in \partial^* \Lambda^{\text{out}}$ we set:

$$T_b \eta(z) = \begin{cases} \eta(z) & \text{if } z \neq x, \\ 0 & \text{if } z = x \end{cases} \tag{1.7}$$

this describes the annihilation of particles along the border;

for $b=(x\to y)\in\partial^*\Lambda^{\text{in}}$ we set:

$$T_b\eta(z)=\begin{cases}\eta(z) & \text{if } z\neq y,\\ 1 & \text{if } z=y\end{cases} \tag{1.8}$$

this describes the creation of particles along the border.

The Kawasaki dynamics is the discrete time Markov chain $(\eta_t)_{t\in\mathbb{N}}$ on state space $\mathcal{X}$ given by the following transition probabilities: for $\eta\neq\eta'$:

$$P(\eta,\eta')=\begin{cases}|\bar\Lambda^{*,\text{orie}}|^{-1}e^{-\beta[H(\eta')-H(\eta)]_+} & \text{if } \exists b\in\bar\Lambda^{*,\text{orie}}:\eta'=T_b\eta,\\ 0 & \text{otherwise}\end{cases} \tag{1.9}$$

and $P(\eta,\eta)=1-\sum_{\eta'\neq\eta}P(\eta,\eta')$, where $[a]_+=a\vee 0$. This is a standard Metropolis dynamics with an open boundary: along each bond touching $\partial^-\Lambda$ from the outside, particles are created with rate $\rho=e^{-\Delta\beta}$ and are annihilated with rate 1, while inside Λ_0 particles are conserved. Note that an exchange of occupation numbers inside the ring $\Lambda\setminus\Lambda_0$ does not involve any change in energy.

It is easy to verify that the stochastic dynamics defined by (1.9) is reversible w.r.t. Gibbs measure corresponding to H.

We will denote by $\mathbb{P}_{\eta_0}$ the probability law of the Markov process $(\eta_t)_{t\geqslant 0}$ starting at η_0 and by $\mathbb{E}_{\eta_0}$ the corresponding expectation.

1.3. Definitions and Notation

In the sequel we use italic capital letters for subsets of Λ, script capital letters for subsets of $\mathcal{X}$, and boldface capital letters for events under the Kawasaki dynamics. We use this convention in order to keep the various notations apart.

In order to formulate our main results in Theorems 1 and 3, we need some definitions.

1. Free particles and clusterized component

Suppose that the finite box $\Lambda\subset\mathbb{Z}^2$ is sufficiently large.

- For $x\in\Lambda_0$, let $nn(x)=\{y\in\Lambda_0:\ |y-x|=1\}$ be the set of nearest–neighbor sites of x in Λ_0.
- A *free particle* in $\eta\in\mathcal{X}$ is a site $x\in\eta\cap\partial^-\Lambda$ or a site $x\in\eta\cap\Lambda_0$ such that $\sum_{y\in nn(x)\cap\Lambda_0}\eta(y)=0$, i.e., a particle not in interaction with any other particle (remember from (1.2) that particles in the interior boundary $\partial^-\Lambda$ have no interaction with other particles).

We denote by η_{fp} the union of free particles in $\partial^- \Lambda$ and free particles in Λ_0 and by η_{cl} the clusterized part of η

$$\eta_{\text{cl}} := \eta \cap \Lambda_0 \setminus \eta_{\text{fp}}. \tag{1.10}$$

2. Clusters, projections, and vacancies

Next we introduce a geometric description of the configurations in terms of contours.

- Given a configuration $\eta \in \mathcal{X}$, consider the set $C(\eta_{\text{cl}}) \subset \mathbb{R}^2$ defined as the union of the 1×1 closed squares centered at the occupied sites of η_{cl} in Λ_0. The maximal connected components $C_1, \ldots, C_m$ $(m \in \mathbb{N})$ of $C(\eta_{\text{cl}})$ are called *clusters* of η. There is a one-to-one correspondence between configurations $\eta_{\text{cl}} \subset \Lambda_0$ and sets $C(\eta_{\text{cl}})$. A configuration $\eta \in \mathcal{X}$ is characterized by a set $C(\eta_{\text{cl}})$, depending only on $\eta \cap \Lambda_0$, plus possibly a set of free particles in $\partial^- \Lambda$ and in Λ_0. We are actually identifying three different objects: $\eta \in \mathcal{X}$, its support $\text{supp}(\eta) \subset \Lambda$, and the pair $(C(\eta_{\text{cl}}), \eta_{\text{fp}})$; we write $x \in \eta$ to indicate that η has a particle at $x \in \Lambda$.

- For $\eta \in \mathcal{X}$, let $|\eta|$ be the number of particles in η, $\gamma(\eta)$ the Euclidean boundary of $C(\eta_{\text{cl}})$, $\gamma(\eta) = \partial C(\eta_{\text{cl}})$; we denote by $g_1(\eta)$ $(g_2(\eta))$ one half of the horizontal (vertical) length of $\gamma(\eta)$, i.e., one half of the number of horizontal (vertical) broken bonds in η_{cl}. Then the energy associated with η is given by

$$H(\eta) = -(U_1 + U_2 - \Delta)|\eta_{\text{cl}}| + U_1 g_2(\eta) + U_2 g_1(\eta) + \Delta|\eta_{\text{fp}}|. \tag{1.11}$$

The maximal connected components of $\partial C(\eta_{\text{cl}})$ are called *contours* of η.

- Let $p_1(\eta)$ and $p_2(\eta)$ be the total lengths of horizontal and vertical projections of $C(\eta_{\text{cl}})$, respectively. More precisely let $r_{j,1} = \{x \in \mathbb{Z}^2 : (x)_1 = j\}$ be the jth column and $r_{j,2} = \{x \in \mathbb{Z}^2 : (x)_2 = j\}$ be the jth row, where $(x)_1$ or $(x)_2$ denote the first or second component of x. We say that a line $r_{j,1}$ $(r_{j,2})$ is *active* if $r_{j,1} \cap C(\eta_{\text{cl}}) \neq \emptyset$ $(r_{j,2} \cap C(\eta_{\text{cl}}) \neq \emptyset)$.
Let

$$\pi_1(\eta) := \{j \in \mathbb{Z} : r_{j,1} \cap C(\eta_{\text{cl}}) \neq \emptyset\} \tag{1.12}$$

and $p_1(\eta) := |\pi_1(\eta)|$. In a similar way we define the vertical projection $\pi_2(\eta)$ and $p_2(\eta)$. We also call $\pi_1(\eta)$ and $\pi_2(\eta)$ the horizontal and vertical *shadows* of η_{cl}, respectively.

Note that $g_1, g_2, \pi_1, \pi_2, p_1, p_2$ are actually depending on η only through η_{cl}, even though, for notational convenience, we omit the subscript cl in their functional dependence.
Note that η_{cl} is not necessarily a connected set and so both the horizontal and vertical projections $\pi_1(\eta)$, $\pi_2(\eta)$ are not in general connected. We have obviously:

$$g_i'(\eta) := g_i(\eta) - p_i(\eta) \geqslant 0. \tag{1.13}$$

- A single cluster C is called *monotonic* if $g_i(C) = p_i(C)$ for $i = 1, 2$, i.e., g_1 and g_2 equal, respectively, the horizontal and vertical side lengths of the rectangle $R(C)$ circumscribed to the unique cluster C. More generally, we call *monotonic* a configuration such that $g_i(\eta) = p_i(\eta)$ for $i = 1, 2$.
- We write

$$\begin{aligned} s(\eta) &:= p_1(\eta) + p_2(\eta), \\ v(\eta) &:= p_1(\eta) p_2(\eta) - |\eta_{\mathrm{cl}}|, \\ n(\eta) &:= |\eta_{\mathrm{fp}}|. \end{aligned} \tag{1.14}$$

Note that $s(\eta)$ coincides with the semi-perimeter if η is a configuration with a single monotonic cluster. It is immediate to show that $v(\eta)$ is a non-negative integer and that it is equal to zero if η_{cl} has a unique rectangular cluster with semi-perimeter $s(\eta)$; it represents the number of vacancies in η. Define:

$$P_1(\eta) = \bigcup_{j \in \pi_1(\eta)} r_{j,1}, \qquad P_2(\eta) = \bigcup_{j \in \pi_2(\eta)} r_{j,2} \tag{1.15}$$

the minimal unions of columns and rows, respectively, in $\mathbb{Z}^2$ containing η_{cl}. By definition we have

$$P_1(\eta) \cap P_2(\eta) \supseteq \eta_{\mathrm{cl}}, \tag{1.16}$$

where $P_1(\eta) \cap P_2(\eta)$ is, in general, the union of rectangles such that $|P_1(\eta) \cap P_2(\eta)| = p_1(\eta) p_2(\eta)$. The *vacancies* of η are the sites in $P_1(\eta) \cap P_2(\eta) \backslash \eta_{\mathrm{cl}}$.

3. Paths, boundaries, and hitting times

A *path* ω is a sequence $\omega = \omega_1, \ldots, \omega_k$ ($k \in \mathbb{N}$, $\omega_i \in \mathcal{X}$) with $P(\omega_i, \omega_{i+1}) > 0$ for $i = 1, \ldots, k-1$. We write $\omega\colon\ \eta \to \eta'$ to denote a path from η to η', namely with $\omega_1 = \eta$ and $\omega_k = \eta'$. A set $\mathcal{A} \subset \mathcal{X}$ with $|\mathcal{A}| > 1$ is *connected* if

and only if for all $\eta, \eta' \in \mathcal{A}$ there exists a path $\omega\colon\ \eta \to \eta'$ such that $\omega_i \in \mathcal{A}$ for all i.

Given a non-empty set $\mathcal{A} \subset \mathcal{X}$, define its *external and internal boundary* as, respectively,

$$\partial^+ \mathcal{A} = \{\zeta \notin \mathcal{A}\colon\ P(\zeta, \eta) > 0 \text{ for some } \eta \in \mathcal{A}\}, \tag{1.17}$$

$$\partial^- \mathcal{A} = \{\zeta \in \mathcal{A}\colon\ P(\zeta, \eta) > 0 \text{ for some } \eta \notin \mathcal{A}\}, \tag{1.18}$$

$$\partial \mathcal{A} := \{(\bar{\eta}, \eta) : \bar{\eta} \in \partial^- \mathcal{A},\ \eta \in \partial^+ \mathcal{A} \text{ with } P(\bar{\eta}, \eta) > 0\} \tag{1.19}$$

that is the set of moves exiting from $\mathcal{A}$.

We define

$$H_{\min}(\partial \mathcal{A}) := \min_{(\bar{\eta}, \eta) \in \partial \mathcal{A}} [H(\bar{\eta}) \vee H(\eta)] \tag{1.20}$$

and we denote by $(\partial \mathcal{A})_{\min}$ the subset of $\partial \mathcal{A}$ where this minimum is realized:

$$(\partial \mathcal{A})_{\min} := \{(\bar{\eta}, \eta) \in \partial \mathcal{A}\colon\ H(\bar{\eta}) \vee H(\eta) = H_{\min}(\partial \mathcal{A})\}. \tag{1.21}$$

Given a non-empty set $\mathcal{A} \subset \mathcal{X}$, define the *first hitting time of* $\mathcal{A}$ as

$$\tau_{\mathcal{A}} = \min\{t \geqslant 0\colon\ \eta_t \in \mathcal{A}\}. \tag{1.22}$$

4. Foliation of $\mathcal{X}$

The configuration space $\mathcal{X}$ can be partitioned as

$$\mathcal{X} = \bigcup_{s=0}^{|\Lambda|} \mathcal{V}_s, \tag{1.23}$$

where

$$\mathcal{V}_s = \{\eta \in \mathcal{X}\colon\ p_1(\eta) + p_2(\eta) = s\} \tag{1.24}$$

is the set of configurations with the sum of the shadows equal to s, called the *s-manifold*.

5. Minimax, saddles, and gates

- The *bottom* $\mathcal{F}(\mathcal{A})$ of a non-empty set $\mathcal{A} \subset \mathcal{X}$ is the set of global minima of the Hamiltonian H in $\mathcal{A}$:

$$\mathcal{F}(\mathcal{A}) = \left\{ \eta \in \mathcal{A} \colon\ H(\eta) = \min_{\zeta \in \mathcal{A}} H(\zeta) \right\}. \tag{1.25}$$

For a set $\mathcal{A}$ whose points have the same energy, we denote (by an abuse of notation) this energy by $H(\mathcal{A})$.

- Given a function $f : \mathcal{X} \to \mathbb{R}$ and a subset $\mathcal{A} \subseteq \mathcal{X}$, we denote by

$$\arg\max_{\mathcal{A}} f := \left\{ \eta \in \mathcal{A} \colon\ f(\eta) = \max_{\xi \in \mathcal{A}} f(\xi) \right\} \tag{1.26}$$

the set of points where the maximum of f in $\mathcal{A}$ is reached.

- The *communication height* between a pair $\eta, \eta' \in \mathcal{X}$ is

$$\Phi(\eta, \eta') = \min_{\omega \colon\ \eta \to \eta'} \max_{\zeta \in \omega} H(\zeta). \tag{1.27}$$

- We call *stability level* of a state $\zeta \in \mathcal{X}$ the energy barrier

$$V_\zeta := \Phi(\zeta, \mathcal{I}_\zeta) - H(\zeta), \tag{1.28}$$

where $\mathcal{I}_\zeta$ is the set of states with energy below $H(\zeta)$:

$$\mathcal{I}_\zeta := \{ \eta \in \mathcal{X} \colon H(\eta) < H(\zeta) \}. \tag{1.29}$$

We set $V_\zeta := \infty$ if $\mathcal{I}_\zeta$ is empty.

- We call *set of V-irreducible states* the set of all states with stability level larger than V:

$$\mathcal{X}_V := \{ \eta \in \mathcal{X} \colon \quad V_\eta > V \}. \tag{1.30}$$

- The *set of stable states* is the set of the global minima of the Hamiltonian

$$\mathcal{X}^s := \mathcal{F}(\mathcal{X}). \tag{1.31}$$

- The set of *metastable states* is given by

$$\mathcal{X}^{\mathrm{m}} := \left\{ \eta \in \mathcal{X} : \quad V_\eta = \max_{\zeta \in \mathcal{X} \setminus \mathcal{X}^{\mathrm{s}}} V_\zeta \right\}. \tag{1.32}$$

- We denote by $(\eta \to \eta')_{\mathrm{opt}}$ the *set of optimal paths* i.e. the set of all paths from η to η' realizing the min–max in $\mathcal{X}$, i.e.

$$(\eta \to \eta')_{\mathrm{opt}} := \left\{ \omega : \eta \to \eta' \ \text{ s.t. } \max_{\xi \in \omega} H(\xi) = \Phi(\eta, \eta') \right\}. \tag{1.33}$$

- The set of *minimal saddles* between $\eta, \eta' \in \mathcal{X}$ is defined as

$$\mathcal{S}(\eta, \eta') = \left\{ \zeta \in \mathcal{X} : \ \exists \omega \in (\eta \to \eta')_{\mathrm{opt}}, \ \ \omega \ni \zeta : \ \max_{\xi \in \omega} H(\xi) = H(\zeta) \right\}. \tag{1.34}$$

- Given a pair $\eta, \eta' \in \mathcal{X}$, we say that $\mathcal{W} \equiv \mathcal{W}(\eta, \eta')$ is a *gate* for the transition $\eta \to \eta'$ if $\mathcal{W}(\eta, \eta') \subseteq \mathcal{S}(\eta, \eta')$ and $\omega \cap \mathcal{W} \neq \emptyset$ for all $\omega \in (\eta \to \eta')_{\mathrm{opt}}$.

- We say that $\mathcal{W}$ is a *minimal gate* for the transition $\eta \to \eta'$ if it is a gate and for any $\mathcal{W}' \subset \mathcal{W}$ there exists $\omega' \in (\eta \to \eta')_{\mathrm{opt}}$ such that $\omega' \cap \mathcal{W}' = \emptyset$. In words, a minimal gate is a minimal (by inclusion) subset of $\mathcal{S}(\eta, \eta')$ that is visited by all optimal paths.

6. Standard and domino rectangles

- We denote by $\mathcal{R}(l_1, l_2)$ the set of configurations whose single contour is a rectangle $R(l_1, l_2)$, with $l_1, l_2 \in \mathbb{N}$. For any $\eta, \eta' \in \mathcal{R}(l_1, l_2)$ we have immediately

$$H(\eta) = H(\eta') = H(\mathcal{R}(l_1, l_2)) = U_1 l_2 + U_2 l_1 - \varepsilon l_1 l_2, \tag{1.35}$$

where

$$\varepsilon := U_1 + U_2 - \Delta. \tag{1.36}$$

- A configuration η is *s-minimal* if it minimizes the energy in $\mathcal{V}_s$, i.e., if it belongs to $\mathcal{F}(\mathcal{V}_s)$

- Let

$$\bar{l} = \left\lceil \frac{U_1 - U_2}{U_1 + U_2 - \Delta} \right\rceil, \tag{1.37}$$

where $\lceil\ \rceil$ denotes the integer part plus 1. For $x \in \mathbb{Z}$, $n \in \mathbb{N}$ we denote as $[x]_n$ the class x mod n in $\mathbb{Z}_n$. For any $s > \bar{l} + 2$, if s has the same parity as $\bar{l}$ i.e., $[s - \bar{l}]_2 = [0]_2$, then we define the set of *0-standard rectangles* as $\mathcal{R}^{0\text{-st}}(s) = \mathcal{R}(\ell_1(s), \ell_2(s))$ with $\ell_1(s) - \ell_2(s) = \bar{l}$, i.e., the set of rectangles with sides

$$\ell_1(s) = \frac{s + \bar{l}}{2}, \qquad \ell_2(s) = \frac{s - \bar{l}}{2} \quad \text{for } [s - \bar{l}]_2 = [0]_2. \tag{1.38}$$

If s has the same parity as $\bar{l} - 1$ i.e., $[s - \bar{l}]_2 = [1]_2$, we define the set of *1-standard rectangles* as $\mathcal{R}^{1\text{-st}}(s) = \mathcal{R}(\ell_1(s), \ell_2(s))$ with $\ell_1(s) - \ell_2(s) = \bar{l} - 1$, i.e., the rectangles with side lengths

$$\ell_1(s) = \frac{s + \bar{l} - 1}{2}, \qquad \ell_2(s) = \frac{s - \bar{l} + 1}{2} \quad \text{for } [s - \bar{l}]_2 = [1]_2 \tag{1.39}$$

and for this value of s we call *quasi standard* and denote by $\mathcal{R}^{\text{q-st}}(s)$, the rectangles.
We set

$$\mathcal{R}^{\text{st}}(s) = \begin{cases} \mathcal{R}^{0\text{-st}}(s) & \text{if } [s - \bar{l}]_2 = [0]_2, \\ \mathcal{R}^{1\text{-st}}(s) & \text{if } [s - \bar{l}]_2 = [1]_2. \end{cases} \tag{1.40}$$

- Let $2 \leqslant l_2 \leqslant \bar{l}$. A rectangle $R(l_1, l_2)$ with $l_1 = 2l_2$ is called 0-domino whereas one with $l_1 = 2l_2 - 3$ is called 0quasi-domino. In both cases $s = l_1 + l_2$ is such that $[s]_3 = [0]_3$. We denote by $\mathcal{R}^{0\text{-dom}}(s)$ ($\mathcal{R}^{0q\text{-dom}}(s)$) the set of 0-domino rectangles (0quasi-domino rectangles) with semiperimeter s.

Similarly a rectangle $R(l_1, l_2)$ with $l_1 = 2l_2 - 2$ is called 1-domino and one with $l_1 = 2l_2 + 1$ called 1quasi-domino. In both cases the semiperimeter s is such that $[s]_3 = [1]_3$. The sets of these rectangles are denoted by $\mathcal{R}^{1\text{-dom}}(s)$ and $\mathcal{R}^{1\text{q-dom}}(s)$), respectively.

A rectangle $R(l_1, l_2)$ with $l_1 = 2l_2 - 1$ is called 2-domino. In this case $[s]_3 = [2]_3$, and the set of these rectangles is denoted by $\mathcal{R}^{2\text{-dom}}(s)$.

As it will be clear in Section 2.2; we do not need to introduce 2quasi-domino rectangles (see Fig. 7). Note that for each $s \in [4, 3\bar{l}]$ there exists n-domino rectangles with n such that $[s]_3 = [n]_3$. If s is such that $n = 1, 0$ then there exists also a $n$quasi-domino rectangle.

1.4. Main Results

Let

$$\underline{0}=\{\eta\in\mathcal{X}:\ \eta(x)=0\,\forall x\in\Lambda\} \tag{1.41}$$

be the configuration with Λ empty and

$$\underline{1}=\{\eta\in\mathcal{X}:\ \eta(x)=1\quad\forall x\in\Lambda_0,\qquad \eta(x)=0\quad\forall x\in\Lambda\backslash\Lambda_0\} \tag{1.42}$$

be the configuration with Λ_0 full and $\Lambda\backslash\Lambda_0$ empty.
We define:

$$l_1^*=\left\lceil\frac{U_1}{U_1+U_2-\Delta}\right\rceil,\qquad l_2^*=\left\lceil\frac{U_2}{U_1+U_2-\Delta}\right\rceil, \tag{1.43}$$

$$s^*:=l_1^*+l_2^*-1, \tag{1.44}$$

and

$$\begin{aligned}\mathcal{P}:=\{\eta:\ &n(\eta)=1,\ v(\eta)=\ell_2(s^*)-1,\ \eta_{\mathrm{cl}}\text{ is connected, monotonic,}\\ &\text{with circumscribed rectangle in }\mathcal{R}(\ell_1(s^*)+1,\ell_2(s^*))\}\end{aligned} \tag{1.45}$$

with $l_i(s)$, $i=1,2$ defined as in (1.38) and (1.39) (recall (1.14)). See Fig. 1 for an example of configuration in $\mathcal{P}$. From (3.7), it follows that $H(\eta)$ is constant on $\mathcal{P}$. We write

$$\begin{aligned}\Gamma:=\ &H(\mathcal{P})-H(\underline{0})=H(\mathcal{P})=U_1l_2^*+U_2(l_1^*-1)\\ &-(U_1+U_2-\Delta)l_2^*(l_1^*-1)+2\Delta-U_1.\end{aligned} \tag{1.46}$$

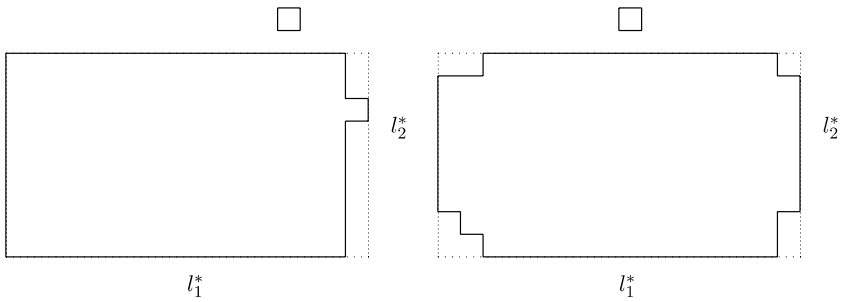

Fig. 1. Configurations in $\mathcal{P}$.

We introduce the following times:

$$\theta_{\underline{0},\underline{1}} = \max\{t < \tau_{\underline{1}} : \eta_t = \underline{0}\}, \tag{1.47}$$

$$\theta_{\underline{0},\mathcal{P},\underline{1}} = \min\{t > \theta_{\underline{0},\underline{1}} : \eta_t \in \mathcal{P}\}. \tag{1.48}$$

As discussed heuristically in Section 2, the behavior of the model strongly depends on the different values of the parameters. We will not actually consider all the possible cases and we will not be interested in giving here the full parameter regime for which our results hold. We will assume:

$$0 < \varepsilon \ll U_2 \quad \text{and} \quad U_2 < U_1 < 2U_2 - 2\varepsilon, \tag{1.49}$$

where $\ll$ means sufficiently smaller; for instance $\varepsilon \leqslant U_2/100$ is enough. Note that this is not a significant restriction since the case of large values of the critical sizes l_1^*, l_2^* is the relevant case from a physical point of view. The isotropic case $U_1 = U_2$ has been already treated in refs. 8 and 6.

The main results about the asymptotics of the tunnelling time and the gate to stability are contained in the following:

Theorem 1. Let U_1, U_2, Δ be such that $U_2/(U_1 + U_2 - \Delta)$ is not integer and (1.49) holds. Let Λ be a box with side $L + 2$. For L sufficiently large and for any $\delta > 0$,

$$\lim_{\beta \to \infty} P_{\underline{0}}\left(e^{\beta(\Gamma - \delta)} \leqslant \tau_{\underline{1}} \leqslant e^{\beta(\Gamma + \delta)}\right) = 1, \tag{1.50}$$

$$\lim_{\beta \to \infty} \frac{1}{\beta} \log \mathbb{E}_{\underline{0}} \tau_{\underline{1}} = \Gamma, \tag{1.51}$$

and moreover if we define $T_\beta := \inf\{n \geqslant 1 : \mathbb{P}_{\underline{0}}(\tau_{\underline{1}} \leqslant n) \geqslant 1 - e^{-1}\}$ then,

$$\lim_{\beta \to \infty} \mathbb{P}_{\underline{0}}(\tau_{\underline{1}} > t T_\beta) = e^{-t} \tag{1.52}$$

and

$$\lim_{\beta \to \infty} \frac{\mathbb{E}_{\underline{0}}(\tau_{\underline{1}})}{T_\beta} = 1. \tag{1.53}$$

Theorem 2. Let U_1, U_2, Δ be such that $U_2/(U_1+U_2-\Delta)$ is not integer and (1.49) holds. Let Λ be a box with side $L+2$. For L sufficiently large,

$$\lim_{\beta\to\infty} P_{\underline{0}}\big(\theta_{\underline{0},\underline{1}} < \theta_{\underline{0},\mathcal{P},\underline{1}} < \tau_{\underline{1}}\big) = 1. \tag{1.54}$$

Theorem 3. Let U_1, U_2, Δ be such that $U_2/(U_1+U_2-\Delta)$ is not integer and (1.49) holds. Let Λ be a box with side $L+2$ and let $\mathcal{R}^{\leqslant(l_1,l_2)}$ ($\mathcal{R}^{\geqslant(l_1,l_2)}$) be the set of configurations whose single contour is a rectangle contained in (containing) a rectangle with sides l_1, l_2. Then, for L sufficiently large,

$$\begin{aligned} &\text{if} \quad \eta\in\mathcal{R}^{\leqslant}(l_1^*-1, l_2^*-1) \Longrightarrow \lim_{\beta\to\infty} \mathbb{P}_\eta(\tau_{\underline{0}} < \tau_{\underline{1}}) = 1, \\ &\text{if} \quad \eta\in\mathcal{R}^{\geqslant}(l_1^*, l_2^*) \Longrightarrow \lim_{\beta\to\infty} \mathbb{P}_\eta(\tau_{\underline{1}} < \tau_{\underline{0}}) = 1. \end{aligned} \tag{1.55}$$

In words, Theorems 1–3 say the following:

- Theorem 1(1.50): For $\beta\to\infty$ the nucleation time from $\underline{0}$ to $\underline{1}$ behaves asymptotically, in probability, as $e^{\Gamma\beta+o(\beta)}$.
- Theorem 1(1.51) and (1.52)): The nucleation time from $\underline{0}$ to $\underline{1}$ has mean value asymptotically given, for large β, by $e^{\Gamma\beta}$ and its distribution, after a suitable rescaling, is asymptotically exponential.
- Theorem 2: The set $\mathcal{P}$ is a gate for the nucleation: all paths from the metastable state $\underline{0}$ to the stable state $\underline{1}$ pass through this set with a probability tending to 1 as $\beta\to\infty$. Note that we do not establish in this theorem the minimality of the gate $\mathcal{P}$ (see definition above), which would involve a much more detailed analysis.
- Theorem 3: l_1^* and l_2^* are the critical sizes, i.e., subcritical rectangles shrink to $\underline{0}$, supercritical rectangles grow to $\underline{1}$.

2. HEURISTICS

2.1. Metastability: Static Heuristics

We will consider the regime

$$\Delta\in(U_1, U_1+U_2), \qquad \beta\longrightarrow\infty, \tag{2.1}$$

which corresponds to a metastable behavior. This is the analogue of the non-conservative case discussed in ref. 9. In the grand-canonical Gibbs

measure the configuration can be represented in terms of spin variables. Indeed, after we make the substitution $\eta(x)=(1+\sigma(x))/2$ in (1.2), where $\sigma(x)\in\{-1,+1\}$ is the spin variable, we can write

$$\begin{aligned} H^{\text{spin}}(\sigma) &= -U_1 \sum_{(x,y)\in\Lambda^*_{0,h}} \frac{1+\sigma(x)}{2}\frac{1+\sigma(y)}{2} \\ &\quad -U_2 \sum_{(x,y)\in\Lambda^*_{0,v}} \frac{1+\sigma(x)}{2}\frac{1+\sigma(y)}{2} - \Delta \sum_{x\in\Lambda_0} \frac{1+\sigma(x)}{2} \\ &= -\frac{U_1}{4} \sum_{(x,y)\in\Lambda^*_{0,h}} \sigma(x)\sigma(y) \\ &\quad -\frac{U_2}{4} \sum_{(x,y)\in\Lambda^*_{0,v}} \sigma(x)\sigma(y) - \left(\frac{U_1+U_2-\Delta}{2}\right)\sum_{x\in\Lambda_0}\sigma(x) + c_1, \end{aligned} \tag{2.2}$$

where c_1 is a constant. Then we have a spin Hamiltonian for anisotropic Ising model (see ref. 9) with pair interaction $J_1=U_1/2$, $J_2=U_2/2$ and magnetic field $h=U_1+U_2-\Delta$.

The metastable behaviour for the non-conservative case in the spin language occurs when $h\in(0, J_1+J_2)$, this corresponds to $\Delta\in((U_1+U_2)/2, U_1+U_2)$. The magnetic field vanishes when $\Delta=U_1+U_2$, which corresponds to the condensation point of the lattice gas. Indeed at this point the density of liquid and gas phase are

$$\rho_{\text{l}}(\beta)=\frac{1+m^*(\beta)}{2}, \qquad \rho_{\text{g}}(\beta)=\frac{1-m^*(\beta)}{2}, \tag{2.3}$$

where $m^*(\beta)$ is the spontaneous magnetization. A perturbative argument based on low-temperature expansion, shows that

$$1-m^*(\beta)=2e^{-2(J_1+J_2)\beta}(1+o(1)), \quad \text{as } \beta\to\infty. \tag{2.4}$$

Indeed $2(J_1+J_2)$ represents the formation energy of a unit square droplet for $h=0$. This, via the identification $J_1=U_1/2$, $J_2=U_2/2$, shows that

$$\rho_{\text{g}}(\beta)=e^{-(U_1+U_2)\beta}[1+o(1)], \quad \text{as } \beta\to\infty. \tag{2.5}$$

This can be identified as the density of the saturated vapor (in the sense of logarithmic equivalence in β). Suppose that we slightly increase the density, avoiding however the appearance of liquid droplets. We can describe

this situation by means of the so-called restricted ensemble (see refs. 2 and 7), namely, the gran-canonical Gibbs measure restricted to a suitable subset of configurations, for instance, where all sufficiently large clusters are suppressed. At low temperature this supersaturated vapor will stay rarefied, so it can be described as pure gas phase with strong mixing properties.

Let us make a rough calculation of the probability to see an $l_1 \times l_2$ droplet of occupied sites centered at the origin. Under restricted ensemble, which we denote by μ^*, we have

$$\mu^*(l_1 \times l_2 \text{ droplet}) \simeq \rho^{l_1 l_2} e^{(U_1+U_2)\beta l_1 l_2 - l_2 U_1 \beta - l_1 U_2 \beta}, \tag{2.6}$$

since ρ is close to the probability to find a particle at a given site and $-U_1$ (resp. $-U_2$) is the binding energy between particles at the neighboring horizontal (resp. vertical) sites. Writing $\rho = e^{-\Delta\beta}$ we obtain

$$\mu^*(l_1 \times l_2 \text{ droplet}) \simeq e^{-\beta[(\Delta - U_1 - U_2) l_1 l_2 + U_1 l_2 + U_2 l_1]}, \tag{2.7}$$

where the exponent has a saddle point at

$$l_1 = \frac{U_1}{U_1 + U_2 - \Delta}, \qquad l_2 = \frac{U_2}{U_1 + U_2 - \Delta}. \tag{2.8}$$

This means that droplets with side length $l_1 < l_1^*$ and $l_2 < l_2^*$ have a probability that decreases in l_1, l_2 and droplets with side length $(l_1, l_2) \geqslant (l_1^*, l_2^*)$ a probability that increases in l_1, l_2. This would leave to the conclusion that l_1^*, l_2^* are the side length of the critical droplet; this is known to be false under Glauber dynamics (see ref. 9), moreover there are heuristic indications that it is also false for Kawasaki dynamics in case of hight anisotropy. This shows how naive is a pure static argumentation. Indeed the dynamical mechanism for the transition between rectangular droplets have an influence in establishing the tendency to grow or shrink.

The choice $\Delta \in (U_1, U_1 + U_2)$ corresponds to $(l_1^*, l_2^*) \in (1, \infty) \times (1, \infty)$, i.e. to a non-trivial critical droplet size.

In physical terms, $\Delta \in (0, U_1)$ represents the unstable gas, $\Delta \in (U_1, U_1 + U_2)$ the metastable gas, $\Delta = U_1 + U_2$ the condensation point, and $\Delta \in (U_1 + U_2, \infty)$ the stable gas.

The most interesting part of the metastable regime is $0 < \varepsilon \ll U_2$ with $\varepsilon = U_1 + U_2 - \Delta$, which corresponds to both l_1^* and l_2^* very large.

2.2. Dynamic Heuristics

What follows is a heuristic discussion aimed to characterize the nucleation pattern. As we said in Section 1 the locally conservative character of our dynamics makes difficult to determine, on rigorous grounds, the tube of typical trajectories realizing the transition from metastability to stability. However, we think that our heuristic arguments are quite convincing but, for a full proof, some more effort is needed.

• **Key transitions**

We start with a coarse graining description: we will restrict ourselves to determine the sequence of rectangles visited by typical trajectories. This is justified since, starting from any configuration, the process will relatively fast go to a rectangle and subsequently it will stay for a long period inside a cycle that plays the role of a generalized basin of attraction of this rectangle. The full tube should also specify the proper interpolation between contiguous rectangles. Our heuristic discussion will also include some information about these interpolations.

By the continuity properties of the dynamics it is reasonable to expect that only transitions between neighboring rectangles have to be taken into consideration.

More precisely, starting from a configuration $\eta \in \mathcal{R}(l_1, l_2)$, with $l_1, l_2 \geqslant 2$, the possible successive rectangles in the tube have to belong to one of the following classes: $\mathcal{R}(l_1+1, l_2)$, $\mathcal{R}(l_1, l_2+1)$, $\mathcal{R}(l_1-1, l_2)$, $\mathcal{R}(l_1, l_2-1)$, $\mathcal{R}(l_1-1, l_2+1)$, and $\mathcal{R}(l_1+1, l_2-1)$. So we shall consider the following transitions:

from $\mathcal{R}(l_1, l_2)$ to $\mathcal{R}(l_1, l_2+1)$, corresponding to vertical growth, that will be denominated *add row* and symbolically denoted by the arrow $\uparrow$ pointing north direction;

from $\mathcal{R}(l_1, l_2)$ to $\mathcal{R}(l_1+1, l_2)$, corresponding to horizontal growth, that will be denominated *add column* and denoted by the arrow $\rightarrow$ pointing east;

from $\mathcal{R}(l_1, l_2)$ to $\mathcal{R}(l_1, l_2-1)$, corresponding to vertical contraction, that will be denominated *remove row* and denoted by the arrow $\downarrow$ pointing south;

from $\mathcal{R}(l_1, l_2)$ to $\mathcal{R}(l_1-1, l_2)$, corresponding to horizontal contraction, that will be denominated *remove column* and denoted by the arrow $\leftarrow$ pointing west;

from $\mathcal{R}(l_1, l_2)$ to $\mathcal{R}(l_1-1, l_2+1)$, corresponding to a readjustment of the edges, making higher and narrower the rectangle by removing a column and simultaneously adding a row. It will be denominated *column to row* and denoted by the arrow $\nwarrow$ pointing northwest;

from $\mathcal{R}(l_1, l_2)$ to $\mathcal{R}(l_1+1, l_2-1)$, corresponding to a readjustment opposite to the previous one. It will be denominated *row to column* and denoted by the arrow $\searrow$ pointing southeast.

The transition from $\mathcal{R}(l_1, l_2)$ to $\mathcal{R}(l_1-1, l_2-1)$ and $\mathcal{R}(l_1+1, l_2+1)$ are not considered as elementary since, as it can be easily seen, a suitable combination of two of the above transitions takes place with larger probability.

At first sight the optimal interpolation paths realizing the above transitions between contiguous rectangles are the ones depicted in Figs. 2–4. Let us call $\Omega^{(1)}$ the set of paths as the one depicted in Fig. 2. They are the natural candidates to realize, in an optimal way, the transition $\uparrow$. For the transition $\rightarrow$ we have an analogous set of paths that we call $\Omega^{(2)}$.

Let us call B the time-reversal operator acting on finite paths; we have for $\omega = \omega_1, \ldots, \omega_T$

$$B\omega = \omega' \quad \text{with } \omega'_i = \omega_{T+1-i} \quad i = 1, \ldots, T. \tag{2.9}$$

For the transition $\downarrow$ we choose the set of paths $\Omega^{(3)}$ obtained by time-reversal from the paths, analogous to the ones in $\Omega^{(1)}$, that realize the transition $\mathcal{R}(l_1-1, l_2)$ to $\mathcal{R}(l_1, l_2)$.

Similarly, for the transition $\leftarrow$ we use the set of paths $\Omega^{(4)}$ obtained by time-reversal from the paths, analogous to the ones in $\Omega^{(2)}$, that realize the transition $\mathcal{R}(l_1, l_2-1)$ to $\mathcal{R}(l_1, l_2)$.

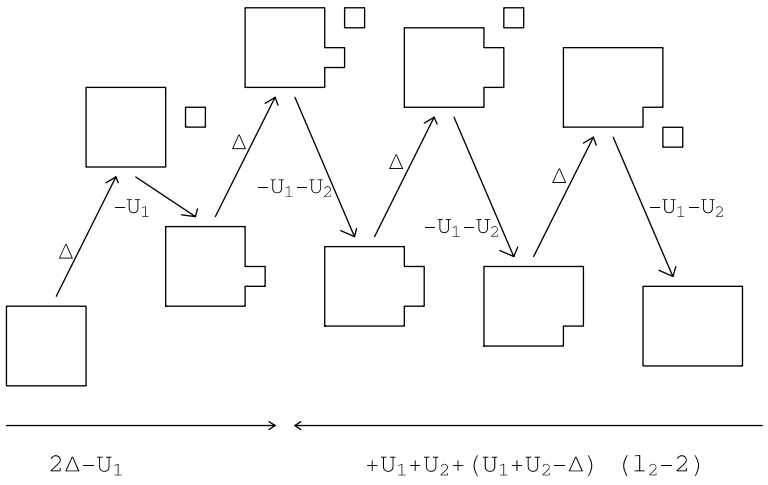

Fig. 2. The procedure to grow a column.

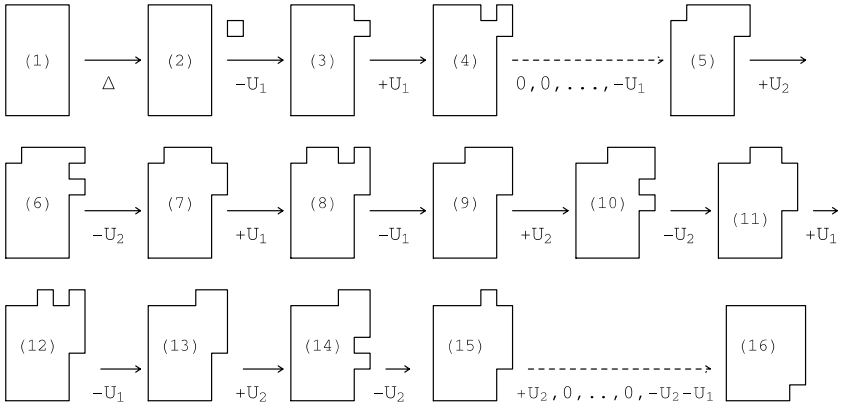

Fig. 3. A path in $\Omega^{(5)}$.

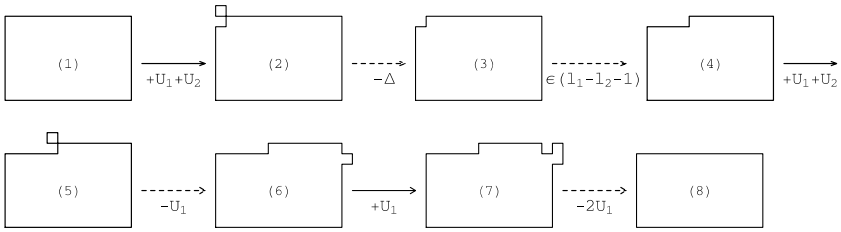

Fig. 4. A path in $\bar{\Omega}^{(5)}$.

The set of paths that we consider as the optimal interpolation for the transition from $\mathcal{R}(l_1, l_2)$ to $\mathcal{R}(l_1 - 1, l_2 + 1)$ in the two cases $l_1 < l_2$, $l_1 \geqslant l_2$, are called $\Omega^{(5)}$ and $\bar{\Omega}^{(5)}$, respectively. A path in $\Omega^{(5)}$ is represented in Fig. 3. where each arrow corresponds to a move and the quantities under the arrows represent the corresponding energy barriers ΔH. Dotted arrows indicate sequences of moves. The maximal energy along the path is reached in the configuration (2). A path in $\bar{\Omega}^{(5)}$ is represented in Fig. 4 where to simplify we indicate under the dotted arrows the sum of the corresponding ΔH. Along this path the maximal energy is reached in configuration (5). In a similar way we define the optimal interpolation paths $\Omega^{(7)}$ and $\bar{\Omega}^{(7)}$ for the transition from $\mathcal{R}(l_1, l_2)$ to $\mathcal{R}(l_1 + 1, l_2 - 1)$. We call *canonical* the paths in the above sets.

Given (l_1, l_2), to determine the most probable transition between $\mathcal{R}(l_1, l_2)$ and one of the previous six contiguous rectangles, we will use the criterion of the smallest energy barrier, defined as the difference between the communication height and $H(\mathcal{R}(l_1, l_2))$. We call *energy barrier from* η

to η' *along the path* $\omega = (\omega_1 = \eta, \ldots, \omega_n = \eta')$ the difference between the maximal height reached along this path and $H(\eta)$. We compute the energy barriers along the canonical paths and we use them to estimate the true energy barriers. We denote by $\Delta H(\text{add row})$ the energy barrier along the paths in $\Omega^{(1)}$; similarly for the other transitions.

From Figs. 2–4 via easy computations, we get:

$$\begin{array}{lll}
\Delta H(\text{add row}) & = 2\Delta - U_2, & \\
\Delta H(\text{add column}) & = 2\Delta - U_1, & \\
\Delta H(\text{remove row}) & = \varepsilon(l_1 - 2) + U_1 + U_2, & \\
\Delta H(\text{remove column}) & = \varepsilon(l_2 - 2) + U_1 + U_2, & \\
\Delta H(\text{row to column}) & = \Delta & \text{if } l_1 < l_2, \\
\Delta H(\text{row to column}) & = U_1 + U_2 + \varepsilon(l_1 - l_2) & \text{if } l_1 \geqslant l_2, \\
\Delta H(\text{column to row}) & = \Delta - U_2 + U_1 & \text{if } l_1 > l_2, \\
\Delta H(\text{column to row}) & = \Delta - U_2 + U_1 + \varepsilon(l_2 - l_1 + 1) & \text{if } l_1 \leqslant l_2.
\end{array} \tag{2.10}$$

These estimated energy barriers are, of course, larger than or equal to the true ones; the equality does not hold in general, since the above canonical paths sometimes happen to be non-optimal. For example, a deeper analysis leads to the conclusion that to add a row, instead of using a path in $\Omega^{(1)}$, it is more convenient to compose $\Omega^{(2)}$ and $\Omega^{(5)}$, resp. $\bar{\Omega}^{(5)}$, when $l_1 < l_2$, resp. $l_1 \geqslant l_2$.

Let us now make a comparison between the estimated energy barriers appearing in equation (2.10). For $l_1 \leqslant l_2$, we can easily check that $\Delta H(\text{row to column}) \leqslant U_1 + U_2 = \Delta + \varepsilon$ is the smallest estimated energy barrier. So in the sequel we will consider only the case $l_1 > l_2$.

For $l_1 > l_2$ we consider two cases:

- $U_1 < 2U_2 - \varepsilon$, that we refer to as "weak anisotropy", where, since

$$\begin{aligned}
&\Delta - U_2 + U_1 < 2\Delta - U_1 < 2\Delta - U_2 \quad \text{and} \\
&U_1 + U_2 + \varepsilon(l_2 - 2) < U_1 + U_2 + \varepsilon(l_1 - 2),
\end{aligned} \tag{2.11}$$

we have only to compare $\Delta H(\text{column to row})$, $\Delta H(\text{remove column})$, and $\Delta H(\text{row to column})$. We have

$$\Delta H(\text{remove column}) < \Delta H(\text{column to row}) \iff l_2 \leqslant \bar{l}, \tag{2.12}$$

$$\Delta H(\text{remove column}) \leqslant \Delta H(\text{row to column}) \iff 2l_2 - 2 \leqslant l_1, \tag{2.13}$$

$$\Delta H(\text{row to column}) < \Delta H(\text{column to row}) \Longleftrightarrow l_1 - l_2 \leqslant \bar{l} - 2. \tag{2.14}$$

Summarizing we have that: in the set $A = \{l_2 \leqslant \bar{l},\ l_1 > 2l_2 - 2\}$ the minimal estimated energy barrier is ΔH(remove column);

in the set $B = \{l_2 > \bar{l},\ l_1 > l_2 + \bar{l} - 2\}$ the minimal estimated energy barrier is ΔH(column to row);

in the set $C = \{l_1 \leqslant l_2 + \bar{l} - 2,\ l_1 < 2l_2 - 2\}$ the minimal estimated energy barrier is ΔH(row to column).

in the set $D = \{l_2 \leqslant \bar{l},\ l_1 = 2l_2 - 2\}$ we have degeneracy of the minimal estimated energy barrier: ΔH(remove column) $=$ ΔH(row to column).

Note that the set C coincides with the set $\{l_2 \leqslant \bar{l},\ l_1 < 2l_2 - 2\} \cup \{l_2 > \bar{l},\ l_1 \leqslant l_2 + \bar{l} - 2\}$, so that $A \cup B \cup C \cup D = \{l_1 > l_2\}$.

We represent $\mathcal{R}(l_1, l_2)$ as points in $\mathbb{Z}^2$ of coordinates l_1, l_2 (representing, respectively, the horizontal and vertical edges). Emerging from any representative point, we plot the arrows corresponding to transitions with minimal ΔH between $\mathcal{R}(l_1, l_2)$ and contiguous rectangles. In Fig. 5 we draw this system of arrows.

Note that the multiplicity of the arrows emerging from a point, corresponding to degeneracy of the minimal ΔH, takes place only in the set D. In the figure the southeast–northwest arrows $\nwarrow\!\!\searrow$ represent the superposition of two arrows $\searrow$ and $\nwarrow$.

- $U_1 > 2U_2 - \varepsilon$, corresponding to "strong anisotropy" where, since

$$\begin{aligned} &2\Delta - U_1 < 2\Delta - U_2,\ 2\Delta - U_1 < \Delta - U_2 + U_1 \quad \text{and} \\ &U_1 + U_2 + \varepsilon(l_2 - 2) < U_1 + U_2 + \varepsilon(l_1 - 2), \end{aligned} \tag{2.15}$$

by (2.10), we deduce that we have only to compare ΔH(remove column), ΔH(add column), and ΔH(row to column). We get

$$\Delta H(\text{remove column}) < \Delta H(\text{add column}) \Longleftrightarrow l_2 < l_2^*, \tag{2.16}$$

$$\Delta H(\text{row to column}) < \Delta H(\text{add column}) \Longleftrightarrow l_1 < l_2 + l_2^* - 2. \tag{2.17}$$

Using 2.13 we have immediately that:

in the set $A' = \{l_2 \leqslant l_2^* - 1,\ l_1 > 2l_2 - 2\}$ the minimal estimated energy barrier is ΔH(remove column);

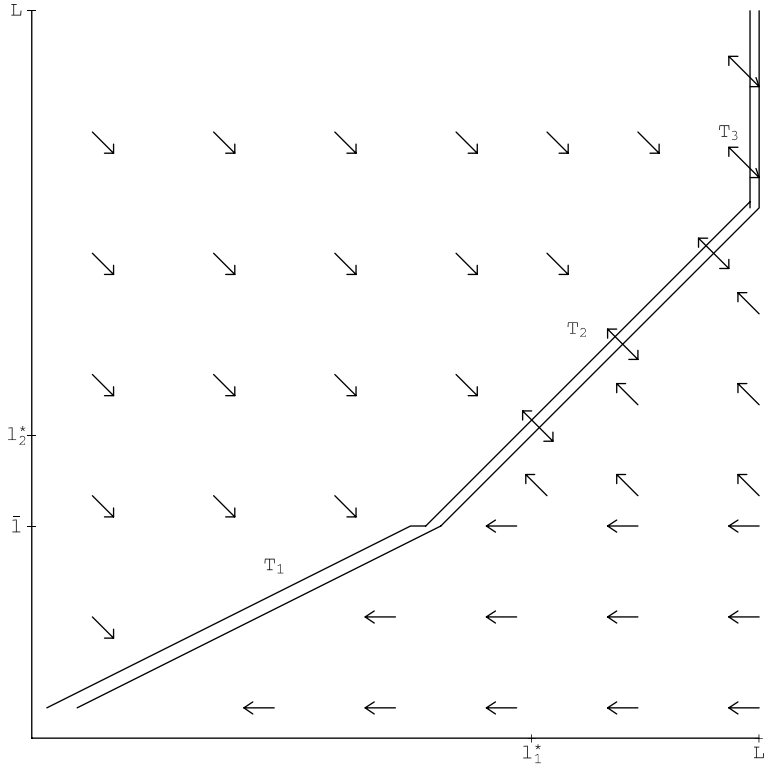

Fig. 5. Weak anisotropy: minimal transitions and tube of typical trajectories.

in the set $B' = \{l_1 < l_2 + l_2^* - 2,\ l_1 < 2l_2 - 2\}$ the minimal estimated energy barrier is ΔH(row to column);

in the set $C' = \{l_2 \geqslant l_2^*,\ l_1 \geqslant l_2 + l_2^* - 2\}$ the minimal estimated energy barrier is ΔH(add column).

in the set $D' = \{l_2 \leqslant l_2^* - 1,\ l_1 = 2l_2 - 2\}$ we have degeneracy of the minimal estimated energy barrier: ΔH(remove column) = ΔH(row to column)

Note that $B' = \{l_2 \leqslant l_2^* - 1,\ l_1 < 2l_2 - 2\} \cup \{l_2 \geqslant l_2^*,\ l_1 < l_2 + l_2^* - 2\}$, so that again $A' \cup B' \cup C' \cup D' = \{l_1 > l_2\}$.

We visualize these results in Fig. 6, using the same graphical representation introduced in the case weak anisotropy.

In the weak anisotropic case, from Fig. 5, it is evident that in the plane (l_1, l_2) there is a region T, represented in the figure, which is attrac-

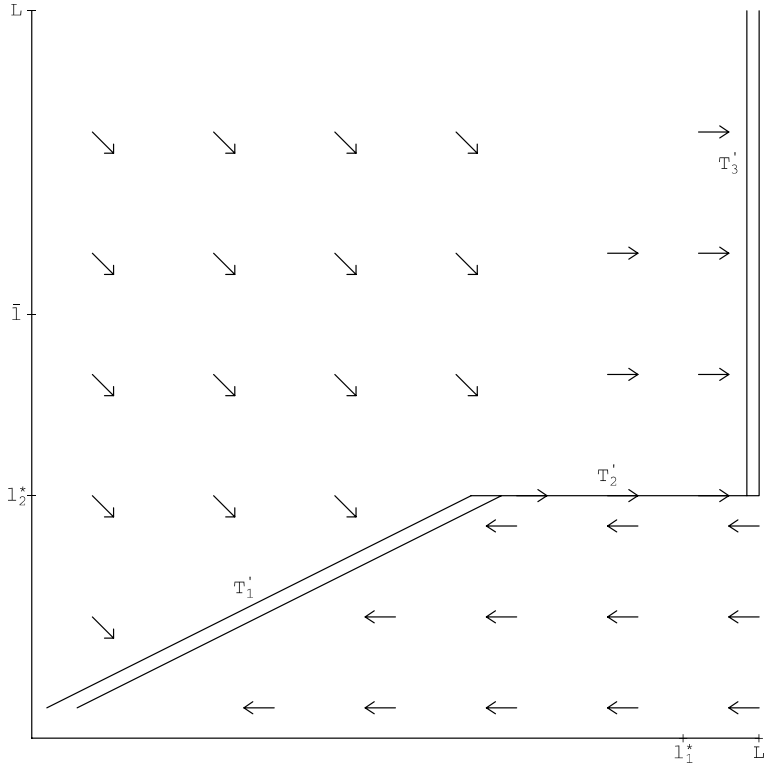

Fig. 6. Strong anisotropy: minimal transitions and tube of typical trajectories.

tive in the sense that if we follow the oriented paths given by the sequences of arrows emerging from every point outside T we end up inside T. The region T consists of three parts: $T_1 = \{(l_1, l_2): l_2 \leqslant \bar{l}$ and $2l_2 - 3 \leqslant l_1 \leqslant 2l_2 - 1\}$ containing domino shape rectangles, $T_2 = \{(l_1, l_2): l_2 > \bar{l}$ and $l_2 + \bar{l} - 1 \leqslant l_1 \leqslant l_2 + \bar{l}\}$ containing standard rectangles (see Section 1.3 point 6) and $T_3 = \{(l_1, l_2): l_1 = L$ and $l_2 \geqslant L - \bar{l}\}$.

Let us now consider the arrows inside the region T. From each $\eta \in T_1$, with $l_1 = 2l_2 - 2$, as a consequence of the degeneracy ΔH(remove column) = ΔH(row to column), we have two exiting arrows, one pointing to $\eta' \in \mathcal{R}(l_1 - 1, l_2)$ and the other pointing to $\eta'' \in \mathcal{R}(l_1 + 1, l_2 - 1)$. Subsequently, starting from η' the minimal estimated ΔH is unique and it corresponds to an arrow pointing to $\mathcal{R}(l_1, l_2 - 1)$; analogously starting from η'' the minimal ΔH is unique and it corresponds to a arrow also pointing to $\mathcal{R}(l_1, l_2 - 1)$ (see Fig. 7).

In T_2, for each value of the semi-perimeter s, there are pairs of configurations (η, η') such that the minimal among the estimated energy barriers

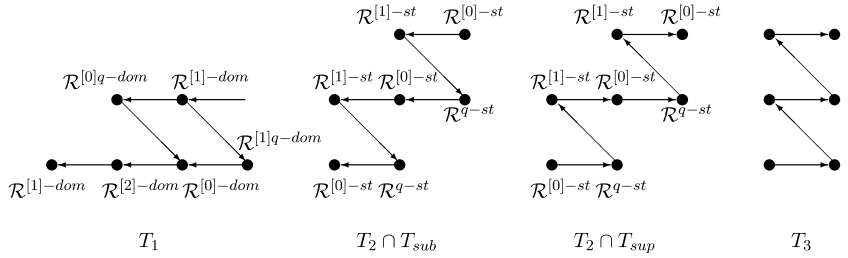

Fig. 7. Minimal transitions inside T_1, T_2 with $l_2 < l_2^*$, T_2 with $l_2 \geqslant l_2^*$ and T_3.

starting from η corresponds to the transition from η to η' and conversely the minimal estimated energy barrier from η' corresponds to the transition from η' to η. So inside T_2 there are pairs of arrows forming two-states loops that we represent as $\nwarrow\!\!\searrow$. This suggests that in T_2 a more detailed study is necessary, based on the analysis of suitable cycles containing the above described loops. These cycles represent a sort of generalized basin of attraction of the standard rectangles contained in the loops: they are the maximal cycles containing a unique standard rectangle. We do not develop in this paper the analysis of these cycles since their structure is quite complicated and they are very big especially close to the critical size (l_1^*, l_2^*). These cycles contain, among others, rectangular configurations and in each cycle all the rectangular configurations have the same semi-perimeter s, i.e., belong to the same manifold $\mathcal{V}_s$. We just make a guess on the transitions leaving these cycles through the points of minimal energy in their boundary; we draw in our picture the arrows between rectangular configurations corresponding to these most probable exits. It turns out that these arrows are horizontal pointing east if $l_2 \geqslant l_2^*$ and pointing west if $l_2 < l_2^*$ (see Fig. 7). In both cases these horizontal arrows point to configurations which are again in the set T, so that we can iterate the argument to analyze all the arrows in T. Thus we associate to the loops $\nwarrow\!\!\searrow$ in the picture cycles containing rectangles in $\mathcal{V}_s$ and transitions given by the horizontal arrows. In T_3 we can argue like in T_2 (see Fig 7).

It is natural at this point to distinguish two parts in the set T: the subcritical part T_{sub} corresponding to T_1 plus the part of T_2 with horizontal arrows pointing west, i.e., with $l_2 < l_2^*$ and the supercritical part T_{sup}, corresponding to the configurations in T_2 with horizontal arrows pointing east, i.e., with $l_2 \geqslant l_2^*$ and T_3.

Let us now summarize our heuristic discussion in the weakly anisotropic case. We expect that every rectangle outside T is attracted by T; the configurations in T_{sub} are subcritical in the sense that they tend to shrink along T following standard or domino shape, depending on l_2; configurations in T_{sup} are supercritical in the sense that they tend to grow

following standard shapes in T_2 and a sequences of rectangles with bases $L-1$ or L in T_3. Moreover to every loop of arrows in T_2 we associate a permanence set containing rectangles in a given manifold $\mathcal{V}_s$.

This heuristical discussion provides a description of the tube of typical nucleating path. Suppose first to consider the typical paths going from the maximal subcritical rectangle to $\underline{0}$. From the discussion on the subcritical part of T_2 we have that the sequence of cycles corresponding to the loops $\nwarrow\!\!\searrow$, connected by the horizontal arrows pointing west define a coarse grained cycle path corresponding to the first part of the tube of typical trajectories going to $\underline{0}$. Looking at T_1 we see that there are no loops there; we can associate to each rectangular configuration η in T_1 the maximal cycle containing η and not containing other rectangular configurations. By using the arrows of the figure we obtain, in this way, a coarse grained cycle path corresponding to the domino part of the tube. The coarse graining of these cycle paths can be resolved by introducing a suitable interpolation between rectangular configurations corresponding to each arrow in the picture, obtaining, in this way a family of true cycle paths, $\mathcal{T}_{\text{sub}}$, describing the tube of typical paths going from the maximal subcritical rectangle to $\underline{0}$.

A similar discussion can be applied to the study of the tube of typical paths going from the minimal supercritical rectangle to $\underline{1}$ obtaining in the same way the family of cycle paths $\mathcal{T}_{\text{sup}}$.

The tube of the typical nucleating paths describing the first excursion from $\underline{0}$ to $\underline{1}$, can be obtained by applying general arguments based on reversibility and by providing a suitable interpolation between the maximal subcritical rectangle and the minimal supercritical one. More precisely to obtain the typical tube from $\underline{0}$ to $\underline{1}$ we apply the time reversal operator B (see (2.9)), to the tube $\mathcal{T}_{\text{sub}}$ and we join it to $\mathcal{T}_{\text{sup}}$ by means of this interpolation. These interpolations between rectangular configurations can be obtained by using the reference path ω^* described in Section 3.2; ω^* can be considered as a representative of typical nucleation path.

Some aspects of the behavior that we have heuristically described are rigorously discussed in this paper; in particular we determine a gate $\mathcal{P}$ for the transition between $\underline{0}$ and $\underline{1}$ (see Theorem 2) and we give a sufficient condition to discriminate subcritical and supercritical standard rectangles (see Theorem 3).

In the strongly anisotropic case, from Fig. 6, it is evident that in the plane (l_1, l_2) there is a connected attractive region T' consisting of three parts $T'_1 = \{(l_1, l_2) : l_2 < l_2^* \text{ and } 2l_2 - 3 \leqslant l_1 \leqslant 2l_2 - 1\} \cup \mathcal{R}(2l_2^* - 3, l^*2)$ containing domino shape rectangles, $T'_2 = \{(l_1, l_2) : l_2 = l_2^* \text{ and } l_2 + l_2^* - 2 \leqslant l_1 < L\}$, and $T'_3 = \{(l_1, l_2) : l_2^* \leqslant l_2 \text{ and } L - 1 \leqslant l_1 \leqslant L\}$.

The properties of T_1' can be discussed in analogy with the weakly anisotropic case. For every configuration in T_2' the minimal estimated energy barrier is $\Delta H(\text{add column})$, which implies that the rectangles in T_2' will indefinitely grow in the horizontal direction until they become a complete horizontal strip with length L. In T_3' the minimal estimated energy barrier is $\Delta H(\text{add row})$, which implies that every horizontal strip with $l_1 = L$ will indefinitely grow in the vertical direction until it covers the whole box.

As in the previous case we can deduce from this discussion a conjecture on the tube of typical paths during the first excursion from $\underline{0}$ to $\underline{1}$.

As far as the strongly anisotropic case is concerned we do not have rigorous results; in particular we do not know any gate for the transition from $\underline{0}$ to $\underline{1}$ but we expect that the first supercritical rectangular configuration is contained in $\mathcal{R}(2l_2^*, l_2^*)$. We can construct, like before, a cycle path $\mathcal{T}'_{\text{sub}}$ describing the tube of typical paths going from the maximal subcritical rectangles in $\mathcal{R}(2l_2^* - 3, l_2^*) \cup \mathcal{R}(2l_2^* - 1, l_2^* - 1)$ to $\underline{0}$ and a cycle path $\mathcal{T}'_{\text{sup}}$ going from the minimal supercritical rectangles in $\mathcal{R}(2l_2^* - 2, l_2^*)$ to $\underline{1}$. Like in the weakly anisotropic case the tube of typical nucleating paths, describing the first excursion from $\underline{0}$ to $\underline{1}$, can be obtained by suitably joining the time-reversed of $\mathcal{T}'_{\text{sub}}$ with $\mathcal{T}'_{\text{sup}}$. Summarizing: the nucleation pattern in the strongly anisotropic case contains a sequence of increasing domino shaped rectangles up to $\mathcal{R}(2l_2^*, l_2^*)$; then a sequence of rectangles with $l_2 = l_2^*$ and l_1 going up to L (the size of the container); finally a sequences of horizontal strips whose width grows from l_2^* to L. We can say that the nucleation pattern, in the strongly anisotropic case, is very similar to the one that we would have for non-conservative Glauber dynamics for *any* anisotropy.

3. PROOF OF THE THEOREMS

The proofs of Theorems 1 and 2 are based on the following results proved in ref. 11 on the asymptotic of tunnelling time and on the gates in the general setup of reversible Markov chains.

Theorem 4. Let $\eta_0 \in \mathcal{X}^{\text{m}}$ and let $\bar{\Gamma}$ be the stability level of the metastable state η_0, i.e., $\bar{\Gamma} := V_{\eta_0}$. Then, for any $\delta > 0$, there exist β_0 and $K > 0$ such that for any $\beta > \beta_0$

$$\mathbb{P}_{\eta_0}(\tau_{\mathcal{X}^{\text{s}}} < e^{\beta(\bar{\Gamma} - \delta)}) < e^{-K\beta}. \tag{3.1}$$

Moreover

$$\lim_{\beta \to \infty} \frac{1}{\beta} \ln \mathbb{P}_{\eta_0}(\tau_{\mathcal{X}^{\text{s}}} > e^{\beta(\bar{\Gamma} + \delta)}) = -\infty \tag{3.2}$$

i.e., this last probability is super-exponentially small in β.

Theorem 5. With η_0 and $\bar{\Gamma}$ as in the hypothesis of Theorem 4, we have:

$$\lim_{\beta\to\infty} \frac{1}{\beta} \log \mathbb{E}_{\eta_0} \tau_{\mathcal{X}^s} = \bar{\Gamma}. \tag{3.3}$$

Moreover, if η_0 is the unique metastable state, $\eta_0 = \mathcal{X}^m$, and if we define $T_\beta := \inf\{n \geqslant 1 : \mathbb{P}_{\eta_0}(\tau_{\mathcal{X}^s} \leqslant n) \geqslant 1 - e^{-1}\}$ then, for any $\delta > 0$,

$$\lim_{\beta\to\infty} \mathbb{P}_{\eta_0}(\tau_{\mathcal{X}^s} > tT_\beta) = e^{-t} \tag{3.4}$$

and

$$\lim_{\beta\to\infty} \frac{\mathbb{E}_{\eta_0}(\tau_{\mathcal{X}^s})}{T_\beta} = 1. \tag{3.5}$$

Theorem 6. For any pair of states η, ξ, for any gate $\mathcal{W} \equiv \mathcal{W}(\eta, \xi) \subseteq \mathcal{S}(\eta, \xi)$ for the transition $\eta \to \xi$, there exists $c > 0$ such that

$$\mathbb{P}_\eta(\tau_{\mathcal{W}} > \tau_\xi) \leqslant e^{-\beta c} \tag{3.6}$$

for sufficiently large β.

Theorems 1 and 2 are an immediate consequence of these results if we prove the following:

(a) $H(\mathcal{P}) =: \Gamma = \Phi(\underline{0}, \underline{1})$,

(b) there exists $\Gamma_0 < \Gamma$ such that $\mathcal{X}_{\Gamma_0} \subseteq \{\underline{0}, \underline{1}\}$,

(c) $\mathcal{P}$ is a gate for the transition $\underline{0} \to \underline{1}$.

Point (a) means that we are able to compute explicitly the communication height between $\underline{0}$ and $\underline{1}$.

Point (b) means that each configuration $\eta \notin \{\underline{0}, \underline{1}\}$ is Γ_0-reducible i.e., we can find a configuration with smaller energy, $\eta' \in \mathcal{I}_\eta$, with $\Phi(\eta, \eta') \leqslant H(\eta) + \Gamma_0$. In other words, there are no too deep wells in the energy landscape, no deeper than the well with bottom $\underline{0}$. We will call *reduction* this step of the proof.

To prove (a) and (c) the general strategy is to find a suitable set of states $\mathcal{B}$ containing $\underline{0}$ and not containing $\underline{1}$ so that $\partial\mathcal{B}$ has to be crossed by

every path going from $\underline{0}$ to $\underline{1}$ (see Section 3.3). Moreover we find a *reference path* $\omega^*: \underline{0} \to \underline{1}$ (see Section 3.2) such that the maximum of the energy in ω^* is reached when crossing $\partial\mathcal{B}$ and this maximal energy in ω^* is equal to $H_{\min}(\partial\mathcal{B})$. As shown in Section 3.4, these two ingredients are sufficient to determine the communication height $\Phi(\underline{0}, \underline{1})$. Moreover by characterizing geometrically the moves producing the crossing of $\partial\mathcal{B}$, we will obtain the gate for the transition $\underline{0} \to \underline{1}$.

In Section 3.5 we will prove point (b) and we will also easily show that (a) and (b) imply that $\bar{\Gamma} := V_{\underline{0}} = \Phi(\underline{0}, \underline{1}) = \Gamma$ and $\underline{0} = \mathcal{X}^{\mathrm{m}}$ and $\underline{1} = \mathcal{X}^{\mathrm{s}}$, (see definitions (1.31) and (1.32)), if the side L of the volume Λ is large enough. Theorems 1 and 2 are therefore immediate consequences of Theorems 4–6.

In Section 3.1 we prove a preliminary result on configurations of minimal energy at given s.

The proof of Theorem 3 is obtained in Section 3.6

3.1. Configurations of Minimal Energy at s Fixed

Lemma 7. For any configuration η:

$$H(\eta) = H(\mathcal{R}(p_1(\eta), p_2(\eta))) + \varepsilon v(\eta) + U_1 g_2'(\eta) + U_2 g_1'(\eta) + n(\eta)\Delta \quad (3.7)$$

with $\varepsilon = U_1 + U_2 - \Delta$ and g_i' defined in (1.13).

Proof.

$$\begin{aligned} H(\eta) &= -U_1 \sum_{(x,y)\in\Lambda_1^*} \eta(x)\eta(y) - U_2 \sum_{(x,y)\in\Lambda_2^*} \eta(x)\eta(y) + \Delta \sum_{x\in\Lambda} \eta(x) \\ &= -(U_1 + U_2) \sum_{x\in\Lambda} \eta_{\mathrm{cl}}(x) + U_1 g_2(\eta) + U_2 g_1(\eta) \\ &\quad + \Delta \sum_{x\in\Lambda} \eta_{\mathrm{cl}}(x) + \Delta n(\eta) \end{aligned} \quad (3.8)$$

by definition of $g_1'(\eta)$, $g_2'(\eta)$ this last expression is given by

$$\begin{aligned} &U_1(p_2(\eta) + g_2'(\eta)) + U_2(p_1(\eta) + g_1'(\eta)) - \varepsilon|\eta_{\mathrm{cl}}| + \Delta n(\eta) \\ &= H(\mathcal{R}(p_1(\eta), p_2(\eta))) + \varepsilon(p_1(\eta)p_2(\eta) - |\eta_{\mathrm{cl}}|) \\ &\quad + U_1 g_2'(\eta) + U_2 g_1'(\eta) + n(\eta)\Delta. \quad \blacksquare \end{aligned} \quad (3.9)$$

We will denote by $p_{\min}(\eta)$ the minimum between $p_1(\eta)$ and $p_2(\eta)$.

The main property of standard rectangles is summarized by the following proposition.

Proposition 8. (a) For all $s > \bar{l} + 2$ a configuration is s-minimal, i.e., it is a configuration of minimal energy in $\mathcal{V}_s$, if and only if it is a standard rectangle in $\mathcal{R}^{\mathrm{st}}(s)$:

$$\mathcal{F}(\mathcal{V}_s) = \mathcal{R}^{\mathrm{st}}(s). \tag{3.10}$$

(b) For all $s > \bar{l} + 2$, the configuration of minimal energy in the set

$$\mathcal{A}(s) := \{\eta \in \mathcal{V}_s : v(\eta) \geqslant p_{\min}(\eta) - 1\} \tag{3.11}$$

are the following:

$$\begin{aligned} \mathcal{F}(\mathcal{A}(s)) = \{\eta \in \mathcal{V}_s &: v(\eta) = \ell_2(s-1) - 1,\ n(\eta) = g_1'(\eta) = g_2'(\eta) = 0 \\ &\text{connected, with circumscribed rectangle in} \\ &\mathcal{R}(\ell_1(s-1) + 1, \ell_2(s-1))\} \end{aligned} \tag{3.12}$$

and consequently we have

$$H(\mathcal{F}(\mathcal{A}(s))) = H(\mathcal{R}^{\mathrm{st}}(s-1)) + \Delta - U_1. \tag{3.13}$$

Proof. To prove (a) we have first to prove that a configuration of minimal energy in $\mathcal{V}_s$ is a single rectangle without free particles; this part of the proof clearly does not require the condition $s > \bar{l} + 2$. Indeed by (3.7), since for any η the quantities $v(\eta), g_1'(\eta), g_2'(\eta), n(\eta)$ are non-negative integers, we have that $H(\eta) \geqslant H(\mathcal{R}(p_1(\eta), p_2(\eta)))$, where the identity holds only if $v(\eta) = g_1'(\eta) = g_2'(\eta) = n(\eta) = 0$. On the other side, $v(\eta) = g_1'(\eta) = g_2'(\eta) = n(\eta) = 0$ implies that η is a unique connected cluster since otherwise, either $g_1'(\eta) + g_2'(\eta) > 0$ or $v(\eta) \geqslant p_1(\eta) \vee p_2(\eta)$. Indeed if we can decouple η into two disconnected components $\eta = \eta_0 \cup (\eta \backslash \eta_0)$ with $g_1'(\eta) + g_2'(\eta) = 0$, then we have that $P_1(\eta_0) \cap P_2(\eta \backslash \eta_0)$ and $P_2(\eta_0) \cap P_1(\eta \backslash \eta_0)$ are vacancies of η, so that the number of vacancies $v(\eta)$ can be estimated by

$$v(\eta) \geqslant |P_1(\eta_0) \cap P_2(\eta \backslash \eta_0)| + |P_2(\eta_0) \cap P_1(\eta \backslash \eta_0)| \geqslant p_1(\eta) \vee p_2(\eta). \tag{3.14}$$

Now if η is a unique connected cluster, since $v(\eta) = 0$, it must coincide with its circumscribed rectangle $R(p_1(\eta), p_2(\eta))$. In conclusion we have

proved that $v(\eta)=g_1'(\eta)=g_2'(\eta)=n(\eta)=0$ if and only if η is a unique rectangle without free particles.

We have to prove now that, to minimize the energy, the rectangular configuration must be a standard rectangle. We will write the energy of a rectangle (see (1.35)) as sum of two functions $H_1(s)$ and $H_2(d)$, where $s=l_1+l_2$ and $d=l_1-l_2$. So, if we substitute in (1.35) $l_1=(s+d)/2$ $l_2=(s-d)/2$, we have

$$H(\mathcal{R}(l_1,l_2))=H_1(s)+H_2(d):=\left[(U_1+U_2)\frac{s}{2}-\frac{\varepsilon}{4}s^2\right]+\left[(U_2-U_1)\frac{d}{2}+\frac{\varepsilon}{4}d^2\right]. \tag{3.15}$$

Since we have to minimize the energy when s is constant we can neglect $H_1(s)$ and minimize the function $H_2(d)$. Indeed, since the difference and the sum of two integers belong to the same parity class, we have:

$$\min_{l_1,l_2\geqslant 1,\ l_1,l_2\in\mathbb{N},\ l_1+l_2=s} H(\mathcal{R}(l_1,l_2))=H_1(s)+\min_{d\in\mathbb{Z},\ |d|\leqslant s-2,\ [d]_2=[s]_2} H_2(d). \tag{3.16}$$

As a function on $\mathbb{R}$, $H_2(d)$ has its minimum in $d_0=(U_1-U_2)/\varepsilon$, $\bar{l}-1<d_0<\bar{l}$. Moreover, its graph is a parabola symmetric w.r.t. the axis $x=d_0$, so $H_2(d):\mathbb{N}\to\mathbb{R}$ has minimum in $d\in\{\bar{l}-1,\bar{l}\}$ (see (1.37)). For any value of $s>\bar{l}+2$ only one of these two values of d is acceptable, the one that has the same parity as s.

For any value of $s>\bar{l}+2$ with $[s]_2=[\bar{l}]_2$ we have $d=\bar{l}$ so that

$$\mathcal{F}(\mathcal{V}_s)=\mathcal{R}\left(\frac{s+\bar{l}}{2},\frac{s-\bar{l}}{2}\right) \tag{3.17}$$

and we note that $\mathcal{R}((s+\bar{l})/2,(s-\bar{l})/2)=\mathcal{R}^{0\text{-st}}(s)$.

In the other case, for any $s>\bar{l}+2$ with $[s]_2\neq[\bar{l}]_2$ we have $d=\bar{l}-1$ so that

$$\mathcal{F}(\mathcal{V}_s)=\mathcal{R}\left(\frac{s+\bar{l}-1}{2},\frac{s-\bar{l}+1}{2}\right) \tag{3.18}$$

and we note that $\mathcal{R}((s+\bar{l}-1)/2,(s-\bar{l}+1)/2)=\mathcal{R}^{1\text{-st}}(s)$.

This concludes the proof of part (a).

To prove (b) we first prove that a configuration of minimal energy in $\mathcal{A}(s+1)$ is a single connected and monotonic cluster without free particles with circumscribed rectangle $R(l_1,l_2)$ with $l_1=p_1(\eta)$ and $l_2=p_2(\eta)$

and $l_1+l_2=s+1$ and with a number of vacancies $v(\eta)=p_{\min}(\eta)-1$. Also in this case, this part of the proof clearly does not require the condition $s>\bar{l}+2$. Indeed by (3.7), since for any η the quantities $g_1'(\eta), g_2'(\eta), n(\eta)$ are non-negative integers and $v(\eta)\geqslant p_{\min}(\eta)-1$, we have that $H(\eta)\geqslant H(R(p_1(\eta), p_2(\eta)))+\varepsilon(p_{\min}(\eta)-1))$, where the identity holds only if $g_1'(\eta)=g_2'(\eta)=n(\eta)=0$ and $v(\eta)=p_{\min}(\eta)-1$.

But in the case $g_1'(\eta)=g_2'(\eta)=n(\eta)=0$ and $v(\eta)=p_{\min}(\eta)-1$, the configuration η is a single connected and monotonic cluster without free particles with circumscribed rectangle $R(l_1, l_2)$ with $l_1=p_1(\eta)$ and $l_2=p_2(\eta)$ and with a number of vacancies $v(\eta)=l_1\wedge l_2-1$. Indeed, as shown in the proof of point (a), if η is not a unique connected cluster, either $g_1'(\eta)+g_2'(\eta)>0$ or $v(\eta)\geqslant p_1(\eta)\vee p_2(\eta)$.

We have now to find the values of the projections l_1 and l_2 minimizing the energy in $\mathcal{A}(s+1)$.

If η is such that $l_1<l_2$ then η cannot minimize the energy in $\mathcal{A}(s+1)$. Indeed we have

$$\begin{aligned} H(\eta) &\geqslant U_1 l_2+U_2 l_1-\varepsilon l_1 l_2+\varepsilon(l_1-1) \\ &> U_1 l_1+U_2 l_2-\varepsilon l_1 l_2+\varepsilon(l_1-1)=H(\eta'), \end{aligned} \tag{3.19}$$

where η' is a configuration given by a rectangle with horizontal side of length l_2-1, and vertical side l_1 plus a protuberance on the vertical side, so that $p_1(\eta')+p_2(\eta')=s+1$ and $v(\eta')=p_{\min}(\eta')-1$.

If η is such that $l_1\geqslant l_2$ then

$$H(\eta)\geqslant U_1 l_2+U_2 l_1-\varepsilon(l_1 l_2-l_2+1)=:\bar{H}(l_1, l_2) \tag{3.20}$$

so that

$$\min_{\eta\in\mathcal{A}(s+1)} H(\eta)\geqslant \min_{l_1+l_2=s+1,\, l_1\geqslant l_2\geqslant 1} \bar{H}(l_1, l_2). \tag{3.21}$$

Defining the new variables $s+1=l_1+l_2$ and $d=l_1-l_2$ if we note that

$$\bar{H}(l_1, l_2)=H_1'(s+1)+H_2'(d), \tag{3.22}$$

where

$$H_1'(s+1)=-\frac{\varepsilon}{4}(s+1)^2+\frac{1}{2}(U_1+U_2+\varepsilon)(s+1)+\varepsilon, \tag{3.23}$$

$$H_2'(d)=\frac{\varepsilon}{4}d^2-\frac{1}{2}(U_1-U_2+\varepsilon)d \tag{3.24}$$

it is sufficient to find the value of d minimizing $H_2'(d)$, since

$$\min_{l_1+l_2=s+1,\, l_1 \geqslant l_2 \geqslant 1} \bar{H}(l_1, l_2) = H_1'(s+1) + \min_{d:[d]_2=[s+1]_2\, 0<d \leqslant s-1} H_2'(d). \tag{3.25}$$

As a function on $\mathbb{R}$, $H_2'(d)$ has its minimum in $d_0+1=((U_1-U_2)/\varepsilon)+1$. Moreover, its graph is a parabola symmetric w.r.t. the axis $x=d_0+1$, so $H_2'(d):\mathbb{N}\to\mathbb{R}$ has minimum in $d=\bar{l}$ or in $d=\bar{l}+1$. For any value of $s>\bar{l}+2$ only one of these two values of d is acceptable, the one that has the same parity as $s+1$.

So for any s with $[s]_2=[\bar{l}]_2$ we have that the minimum is obtained for $d=\bar{l}+1$, corresponding to the values $l_1=(s+1+\bar{l}+1)/2$ and $l_2=(s+1-\bar{l}-1)/2$. Note that $l_1=((s+\bar{l})/2)+1=\ell_1(s)+1$ and $l_2=(s-\bar{l})/2=\ell_2(s)$. Equation (3.25) becomes

$$\begin{aligned}
&\min_{l_1+l_2=s+1,\, l_1 \geqslant l_2 \geqslant 1} \bar{H}(l_1, l_2) \\
&= H\Big(\mathcal{R}\Big(\frac{s+1+\bar{l}+1}{2}, \frac{s+1-\bar{l}-1}{2}\Big)\Big) + \varepsilon\Big(\frac{s+1-\bar{l}-1}{2}-1\Big) \\
&= U_1\Big(\frac{s-\bar{l}}{2}\Big) + U_2\Big(\frac{s+\bar{l}}{2}\Big) + U_2 - \varepsilon\Big[\Big(\frac{s-\bar{l}}{2}\Big)\Big(\frac{s+\bar{l}}{2}\Big)\Big] - \varepsilon \\
&= H\Big(\mathcal{R}^{0\text{-st}}(s)\Big) + U_2 - \varepsilon = H\Big(\mathcal{R}^{0\text{-st}}(s)\Big) + \Delta - U_1.
\end{aligned} \tag{3.26}$$

And for any s with $[s]_2 \neq [\bar{l}]_2$ we have that the minimum is obtained for $d=\bar{l}$, corresponding to the values $l_1=(s+1+\bar{l})/2$ and $l_2=(s+1-\bar{l})/2$. Note that $l_1=((s+\bar{l}-1)/2)+1=\ell_1(s)+1$ and $l_2=(s-\bar{l}+1)/2=\ell_2(s)$. Equation (3.25) becomes

$$\begin{aligned}
\min_{l_1+l_2=s+1,\, l_1 \geqslant l_2 \geqslant 1} \bar{H}(l_1, l_2) &= H\Big(\mathcal{R}\Big(\frac{s+1+\bar{l}}{2}, \frac{s+1-\bar{l}}{2}\Big)\Big) + \varepsilon\Big(\frac{s+1-\bar{l}}{2}-1\Big) \\
&= U_1\Big(\frac{s-\bar{l}+1}{2}\Big) + U_2\Big(\frac{s+\bar{l}-1}{2}\Big) \\
&\quad + U_2 - \varepsilon\Big[\Big(\frac{s-\bar{l}+1}{2}\Big)\Big(\frac{s+\bar{l}-1}{2}\Big)\Big] - \varepsilon \\
&= H(\mathcal{R}^{1\text{-st}}(s)) + \Delta - U_1
\end{aligned} \tag{3.27}$$

that ends the proof of part (b). ∎

3.2. Reference Path

We construct now a particular reference path $\omega^* : \underline{0} \to \underline{1}$ (see proof of theorems 1 and 2). It will be given by a particular sequence of growing domino and standard rectangles, such that the maximum of the energy on ω^*, $\{\arg\ \max_{\omega^*} H\}$, is reached on particular configurations given by a rectangle $R(l_1^* - 1, l_2^*)$ with a protuberance on the shorter side and a free particle.

We will prove in Section 3.4 that $\omega^* \in (\underline{0} \to \underline{1})_{\text{opt}}$ so that $\{\arg\max_{\omega^*} H\} \in \mathcal{S}(\underline{0}, \underline{1})$.

We want to recall here that in this paper we get only a partial solution to the problem of the determination of the tube of typical paths, i.e., the set of paths followed by the process with high probability during the transition from $\underline{0}$ to $\underline{1}$. It is easy to prove that a typical path is in the set $(\underline{0} \to \underline{1})_{\text{opt}}$. Note that this set is much larger than the tube of typical paths; we have a lot of freedom in the construction of the reference path, especially far from its maximal energy value. However, we conjecture that the path ω^*, that we are going to construct, is not only optimal but also it suggests the structure of the tube of typical paths.

The idea of the construction of ω^* is the following: we first construct a skeleton path $\{\bar{\omega}_s\}_{s=2}^{2L}$ given by a sequence of rectangles with semi-perimeter s. For $s \leqslant 3\bar{l}$ these are domino rectangles (of type 0, 1, or 2) and for $s \geqslant 3\bar{l}$ these are standard rectangles (of types 0 or 1). Obviously $\bar{\omega}_s$ is not a path in the sense that the transition from $\bar{\omega}_s$ to $\bar{\omega}_{s+1}$ can not be given in a single step of the dynamics, since $\bar{\omega}_s$ and $\bar{\omega}_{s+1}$ are rectangles. Thus to obtain a path we have to interpolate each transition of the skeleton path $\bar{\omega}$. This is done in two different steps. We first introduce between $\bar{\omega}_s$ and $\bar{\omega}_{s+1}$ a sequence of configurations $\tilde{\omega}_{s,1}, \ldots, \tilde{\omega}_{s,i_s}$ given by $\bar{\omega}_s$ plus a growing row or column; again these configurations are given by a single increasing droplet. This step is non-trivial since, as explained in more detail later on, there are cases in which to grow a row we first grow a column and then we move this column to a new row with a motion along the border of the droplet. Indeed it turns out that this is more convenient from an energetic point of view and this strategy is crucial near the exit from $\mathcal{B}$ (see proof of Theorems 1 and 2). The last interpolation, to obtain from the sequence of configurations $\tilde{\omega}_{s,i}$ a path ω^*, i.e., with $P(\omega_j^*, \omega_{j+1}^*) > 0$, consists in inserting between every couple of consecutive configurations in $\tilde{\omega}$ for which the cluster is increased by one particle, a sequence of configurations with a new particle initially created at the boundary of the box and then brought to the correct site with a sequence of consecutive moves of this free particle.

Skeleton: $\bar{\omega}$.

Let us construct a sequence of rectangular configurations $\bar{\omega} = \{\bar{\omega}_s\}$ with $s = 0, \ldots, 2L$, namely,

$$\bar{\omega}_1 = \underline{0},\ \bar{\omega}_2 = \{x_0\}, \ldots, \bar{\omega}_{2L} = \mathcal{F}(\mathcal{X}) \in \underline{1}, \tag{3.28}$$

where x_0 is a given site in Λ_0 and $\forall s\ \bar{\omega}_s \subset \bar{\omega}_{s+1}$.

Step a. For any $s \leqslant 3\bar{l}$, $\{\bar{\omega}_s\}$ is a growing sequence of domino rectangles, depending on the value of s. Indeed, if $[s]_3 = [0]_3$ in $\mathbb{Z}_3$, i.e., $s = 3l_2$ for some $l_2 \leqslant \bar{l}$, we have $\bar{\omega}_s \in \mathcal{R}(2l_2, l_2)$ is a 0-domino rectangle; if $[s]_3 = [1]_3$ in $\mathbb{Z}_3$, i.e., $s = 3l_2 - 2$ for some l_2, we have $\bar{\omega}_s \in \mathcal{R}(2l_2 - 2, l_2)$ is a 1-domino rectangle; if $[s]_3 = [2]_3$ in $\mathbb{Z}_3$, i.e., $s = 3l_2 - 1$ for some l_2, we have $\bar{\omega}_s \in \mathcal{R}(2l_2 - 1, l_2)$ is a 2-domino rectangle.

Step b. For $3\bar{l} \leqslant s \leqslant 2L - \bar{l}$, $\{\bar{\omega}_s\}$ is a growing sequence of standard rectangles if $[s - \bar{l}]_2 = [0]_2$ in $\mathbb{Z}_2$, i.e., $s = 2l_2 + \bar{l}$ for some $l_2 \geqslant \bar{l}$, we have $\bar{\omega}_s \in \mathcal{R}(l_2 + \bar{l}, l_2)$ is a 0-standard rectangle; if $[s - \bar{l}]_2 = [1]_2$ in $\mathbb{Z}_2$, i.e., $s = 2l_2 + \bar{l} - 1$ for some $l_2 \geqslant \bar{l}$, we have $\bar{\omega}_s \in \mathcal{R}(l_2 + \bar{l} - 1, l_2)$ is a 1-standard rectangle.
Note that if $l_2 = \bar{l}$ the 2-domino and 1-standard shape coincide.

Step c. For $s \geqslant 2L - \bar{l}$, $\{\bar{\omega}_s\} \in \mathcal{R}(L, s - L)$.

First interpolation: $\tilde{\omega}$.

Given a choice for $\bar{\omega}_s$, we can construct the path $\tilde{\omega}_{s,i}$ such that $\tilde{\omega}_{s,0} = \bar{\omega}_s$ and insert between each pair $(\bar{\omega}_s, \bar{\omega}_{s+1})$, $\forall s$ a sequence of configurations $\tilde{\omega}_{s,i}$ for $i = 0, 1, \ldots, i_s$.

Step a.1. If $s \leqslant 3\bar{l}$ and $[s]_3 = [1]_3$ add a vertical column as in Fig. 2 passing from $\tilde{\omega}_{s,0} \in \mathcal{R}(2l_2, l_2 + 1)$ to the 2-domino rectangle $\tilde{\omega}_{s,i_s} \in \mathcal{R}(2l_2 + 1, l_2 + 1)$. More precisely $\tilde{\omega}_{s,1}$ is the configuration obtained creating a particle on the column (as in Fig. 2). We repeat this step for other $l_2 - 1$ particles that are created in the same column, so the configuration $\tilde{\omega}_{s,i_s} \in \mathcal{R}(2l_2 + 1, l_2 + 1)$ is a 2-domino rectangle.

Step a.2. If $s \leqslant 3\bar{l}$ and $[s]_3 = [2]_3$ add a vertical column as in Fig. 2 passing from $\tilde{\omega}_{s,0} \in \mathcal{R}(2l_2 - 1, l_2)$ to $\tilde{\omega}_{s,i_s} \in \mathcal{R}(2l_2, l_2)$ that is a 0-domino rectangle.

Step a.3. If $s \leqslant 3\bar{l}$ and $[s]_3 = [0]_3$ add a vertical column as in Fig. 2 passing from $\tilde{\omega}_{s,0} \in \mathcal{R}(2l_2, l_2)$ to the quasi-domino rectangle $\tilde{\omega}_{s,l_2} \in \mathcal{R}(2l_2 + 1, l_2)$ as described in the previous case a.1. Then use the path described in Fig. 4 to define the path from $\tilde{\omega}_{s,l_2} \in \mathcal{R}(2l_2 + 1, l_2)$ to $\tilde{\omega}_{s,i_s} \in \mathcal{R}(2l_2, l_2 + 1)$ that is a 1-domino rectangle.

For $s \geqslant 3\bar{l}$, we can insert between each pair of standard rectangles $(\bar{\omega}_s, \bar{\omega}_{s+1})$, a sequence of configurations $\tilde{\omega}_{s,i}$ for $i = 0, 1, \ldots, i_s$ as follows.

Step b.1. If $3\bar{l} \leqslant s \leqslant 2L - \bar{l}$ and $[s - \bar{l}]_2 = [1]_2$ we have $\bar{\omega}_s \in \mathcal{R}(l_2 + \bar{l} - 1, l_2)$ for some value of l_2, add a vertical column as in Fig. 2

to obtain $\tilde{\omega}_{s,i_s} \in \mathcal{R}(l_2+\bar{l}, l_2)$ that is a 0-standard rectangle in the same way as described in step a.1.

Step b.2. If $3\bar{l} \leqslant s \leqslant 2L-\bar{l}$ and $[s-\bar{l}]_2=[0]_2$ we have $\bar{\omega}_s \in \mathcal{R}(l_2+\bar{l}, l_2)$, add a vertical column as in Fig. 2 to obtain $\tilde{\omega}_{s,l_2} \in \mathcal{R}(l_2+\bar{l}+1, l_2)$ a quasi-standard rectangle. Then we pass from $\tilde{\omega}_{s,l_2} \in \mathcal{R}(l_2+\bar{l}+1, l_2)$ to $\tilde{\omega}_{s,i_s} \in \mathcal{R}(l_2+\bar{l}, l_2+1)$ that is a 1-standard rectangle using the path described in Fig. 4, in the same way as in step a.3.

Step c.1. Use first the path given by the time-reversal of the one represented in Fig. 4 to define a first interpolation between $\mathcal{R}(L, s-L)=\bar{\omega}_s$ and $\mathcal{R}(L-1, s-L+1)$, and then use the path described in Fig. 2 to add a column to $\mathcal{R}(L-1, s-L+1)$ in order to reach $\mathcal{R}(L, s-L+1)=\bar{\omega}_{s+1}$.

Second interpolation: ω^*.

For any pair of configurations $(\tilde{\omega}_{s,i}, \tilde{\omega}_{s,i+1})$ such that $|\tilde{\omega}_{s,i}| < |\tilde{\omega}_{s,i+1}|$, by construction of the path $\tilde{\omega}_{s,i}$ the particles are created along the external boundary of the clusters. So there exists $x_1, \ldots, x_{j_i}$ a connected chain of nearest–neighbor empty sites of $\tilde{\omega}_{s,i}$ such that $x_1 \in \partial^- \Lambda$ and x_{j_i} is the site where is located the additional particle in $\tilde{\omega}_{s,i+1}$. Define the following:

$$\omega^*_{s,i,0}=\tilde{\omega}_{s,i}, \qquad \omega^*_{s,i,j_i}=\tilde{\omega}_{s,i+1} \quad \forall s=0, \ldots, 2(L+2). \tag{3.29}$$

Insert between each pair $(\tilde{\omega}_{s,i}, \tilde{\omega}_{s,i+1})$, a sequence of configurations $\omega^*_{s,i,j}$, for $j=1, \ldots, j_i-1$, where the free particle is moving from $x_1 \in \partial^- \Lambda$ to the cluster until it reaches the position x_{j_i}.

Otherwise for any pair of configurations $(\tilde{\omega}_{s,i}, \tilde{\omega}_{s,i+1})$ such that $|\tilde{\omega}_{s,i}|=|\tilde{\omega}_{s,i+1}|$, we define $\omega^*_{s,i,0}=\tilde{\omega}_{s,i}$; $\omega^*_{s,i+1,0}=\tilde{\omega}_{s,i+1}$. This conclude the definition of the reference path.

We want now to describe in more details the reference path $\omega^*_{s,i,j}$ near the critical value $s^*=l_1^*+l_2^*-1$.

Proposition 9. If the hypothesis (1.49) holds, we have:

(i) In the reference path ω^* the standard regime starts before s^*:

$$s^* > 3\bar{l}. \tag{3.30}$$

(ii) The standard rectangle with semi-perimeter s^* has sides:

$$\ell_1(s^*)=l_1^*, \quad \ell_2(s^*)=l_2^*-1 \quad \text{if } [s^*-\bar{l}]_2=[0]_2, \tag{3.31}$$

$$\ell_1(s^*)=l_1^*-1, \quad \ell_2(s^*)=l_2^* \quad \text{if} [s^*-\bar{l}]_2=[1]_2. \tag{3.32}$$

(iii) The standard rectangle with semi-perimeter $s^* + 1$ has sides $\ell_1(s^*+1) = l_1^*$ and $\ell_2(s^*+1) = l_2^*$.

(iv) The standard rectangle with semi-perimeter $s^* - 1$ has sides $\ell_1(s^*-1) = l_1^* - 1$ and $\ell_2(s^*-1) = l_2^* - 1$.

(v) The standard rectangle of maximal energy is in $\mathcal{R}^{\mathrm{st}}(s^*)$:

$$\arg \max_{\cup_{s>\bar{l}+2}\mathcal{R}^{\mathrm{st}}(s)} H = \mathcal{R}^{\mathrm{st}}(s^*). \tag{3.33}$$

Proof. Let $(U_1/\varepsilon) =: \left[(U_1/\varepsilon)\right] + \delta_1$ and $(U_2/\varepsilon) =: \left[(U_2/\varepsilon)\right] + \delta_2$. From Eq. (1.43), we can write

$$l_1^* = \frac{U_1}{\varepsilon} + 1 - \delta_1 \quad \text{and} \quad l_2^* = \frac{U_2}{\varepsilon} + 1 - \delta_2. \tag{3.34}$$

Even case. If $0 < \delta_2 \leqslant \delta_1 < 1$:

$$\begin{aligned} \bar{l} &= \left[\frac{U_1}{\varepsilon} - \frac{U_2}{\varepsilon}\right] + 1 = \left[\frac{U_1}{\varepsilon}\right] - \left[\frac{U_2}{\varepsilon}\right] + [\delta_1 - \delta_2] + 1 \\ &= l_1^* - l_2^* + 1 \Longrightarrow [s^* - \bar{l}]_2 = [0]_2. \end{aligned} \tag{3.35}$$

Odd case. If $0 < \delta_1 < \delta_2 < 1$:

$$\begin{aligned} \bar{l} &= \left[\frac{U_1}{\varepsilon} - \frac{U_2}{\varepsilon} + 1\right] \\ &= \left[\frac{U_1}{\varepsilon}\right] - \left[\frac{U_2}{\varepsilon}\right] + [\delta_1 - \delta_2 + 1] = l_1^* - l_2^* \Longrightarrow [s^* - \bar{l}]_2 = [1]_2. \end{aligned} \tag{3.36}$$

Let us prove (i); by (1.49) we have:

$$2l_2^* - l_1^* = 2\frac{U_2}{\varepsilon} + 2 - 2\delta_2 - \frac{U_1}{\varepsilon} - 1 + \delta_1 \geqslant 3 - 2\delta_2 + \delta_1. \tag{3.37}$$

In the even case $[s^* - \bar{l}]_2 = [0]_2$ we have:

$$\begin{aligned} s^* - 3\bar{l} &= l_1^* + l_2^* - 1 - 3l_1^* + 3l_2^* - 3 = 2(2l_2^* - l_1^*) - 4 \\ &\geqslant 2(3 - 2\delta_2 + \delta_1) - 4 \geqslant 2(3 - \delta_2) - 4 > 0. \end{aligned} \tag{3.38}$$

In the odd case $[s^*-\bar{l}]_2=[1]_2$ we have:

$$s^*-3\bar{l}=l_1^*+l_2^*-1-3l_1^*+3l_2^*=2(2l_2^*-l_1^*)-1\geqslant 2(3-2\delta_2+\delta_1)-1>0. \tag{3.39}$$

The proof of (ii), (iii), and (iv) is an immediate consequence of the definitions (1.38) and (1.39).

Indeed in the even case we have:

$$\ell_1(s^*)=\frac{s^*+\bar{l}}{2}=l_1^*,\qquad \ell_2(s^*)=\frac{s^*-\bar{l}}{2}=l_2^*-1, \tag{3.40}$$

$$\ell_1(s^*+1)=\frac{s^*+1+\bar{l}-1}{2}=l_1^*,\qquad \ell_2(s^*+1)=\frac{s^*+1-\bar{l}+1}{2}=l_2^*, \tag{3.41}$$

$$\ell_1(s^*-1)=\frac{s^*-1+\bar{l}-1}{2}=l_1^*-1,\quad \ell_2(s^*-1)=\frac{s^*-1-\bar{l}+1}{2}=l_2^*-1. \tag{3.42}$$

In the odd case we have:

$$\ell_1(s^*)=\frac{s^*+\bar{l}-1}{2}=l_1^*-1,\qquad \ell_2(s^*)=\frac{s^*-\bar{l}+1}{2}=l_2^*, \tag{3.43}$$

$$\ell_1(s^*+1)=\frac{s^*+1+\bar{l}}{2}=l_1^*,\qquad \ell_2(s^*+1)=\frac{s^*+1-\bar{l}}{2}=l_2^*, \tag{3.44}$$

$$\ell_1(s^*-1)=\frac{s^*-1+\bar{l}}{2}=l_1^*-1,\qquad \ell_2(s^*-1)=\frac{s^*-1-\bar{l}}{2}=l_2^*-1. \tag{3.45}$$

To prove (v), by recalling (3.15), since $\ell_1(s)-\ell_2(s)=\bar{l}$ in case $[s^*-\bar{l}]_2=[0]_2$ and $\ell_1(s)-\ell_2(s)=\bar{l}-1$ in case $[s^*-\bar{l}]_2=[1]_2$, we have:

$$\begin{aligned} H(\mathcal{R}^{0\text{-st}}(s)) &= H\Big(\mathcal{R}\Big(\frac{s+\bar{l}}{2},\frac{s-\bar{l}}{2}\Big)\Big)=H_1(s)+H_2(\bar{l})\\ &= \frac{U_1+U_2}{2}s-\frac{\varepsilon}{4}s^2+\frac{U_2-U_1}{2}\bar{l}+\frac{\varepsilon}{4}\bar{l}^2 \quad \text{for } [s-\bar{l}]_2=[0]_2, \end{aligned} \tag{3.46}$$

$$H(\mathcal{R}^{1\text{-st}}(s)) = H\Big(\mathcal{R}\Big(\frac{s+\bar{l}-1}{2}, \frac{s-\bar{l}+1}{2}\Big)\Big) = H_1(s) + H_2(\bar{l}-1)$$
$$= \frac{U_1+U_2}{2}s - \frac{\varepsilon}{4}s^2 + \frac{U_2-U_1}{2}(\bar{l}-1)$$
$$+\frac{\varepsilon}{4}(\bar{l}-1)^2 \quad \text{for } [s-\bar{l}]_2 = [1]_2. \tag{3.47}$$

By maximizing the function $H_1(s) = ((U_1+U_2)/2)s - (\varepsilon/4)s^2$ in $\mathbb{R}$ we obtain the maximum in $s_0 = ((U_1+U_2)/\varepsilon) = l_1^* + l_2^* - 2 + \delta_1 + \delta_2$; moreover, $H_1(s)$ is a parabola symmetric w.r.t. the axis $x = s_0$. We can conclude that the maximal energy of standard rectangles, 0 or 1-standard, for s integer, is obtained for $s \in \{s^*-1, s^*, s^*+1\}$. By a direct comparison we can conclude that this maximal energy is obtained for $s = s^*$. Indeed in case $[s^*-\bar{l}]_2 = [0]_2$ by proposition points (ii), (iii), and (iv) we have $\mathcal{R}^{\text{st}}(s^*) = \mathcal{R}(l_1^*, l_2^*-1)$, $\mathcal{R}^{\text{st}}(s^*-1) = \mathcal{R}(l_1^*-1, l_2^*-1)$ and $\mathcal{R}^{\text{st}}(s^*+1) = \mathcal{R}(l_1^*, l_2^*)$ so that:

$$H(\mathcal{R}^{\text{st}}(s^*)) - H(\mathcal{R}^{\text{st}}(s^*-1)) = U_2 - \varepsilon(l_2^*-1) = \varepsilon\delta_2 > 0, \tag{3.48}$$

$$H(\mathcal{R}^{\text{st}}(s^*)) - H(\mathcal{R}^{\text{st}}(s^*+1)) = -U_1 + \varepsilon l_1^* = \varepsilon(1-\delta_1) > 0. \tag{3.49}$$

In case $[s^*-\bar{l}]_2 = [1]_2$ we have $\mathcal{R}^{\text{st}}(s^*) = \mathcal{R}(l_1^*-1, l_2^*)$, $\mathcal{R}^{\text{st}}(s^*-1) = \mathcal{R}(l_1^*-1, l_2^*-1)$ and $\mathcal{R}^{\text{st}}(s^*+1) = \mathcal{R}(l_1^*, l_2^*)$ so that:

$$H(\mathcal{R}^{\text{st}}(s^*)) - H(\mathcal{R}^{\text{st}}(s^*-1)) = U_1 - \varepsilon(l_1^*-1)\varepsilon\delta_1 > 0, \tag{3.50}$$

$$H(\mathcal{R}^{\text{st}}(s^*)) - H(\mathcal{R}^{\text{st}}(s^*+1)) = -U_2 + \varepsilon l_2^* = \varepsilon(1-\delta_2) > 0. \quad \blacksquare \tag{3.51}$$

We note that, by using point (ii) of the previous Proposition 9, the circumscribed rectangle to the configurations in $\mathcal{P}$, i.e., the rectangle with sides $\ell_1(s^*)+1, \ell_2(s^*)$, is standard only in the case $[s^*-\bar{l}]_2 = [1]_2$. In the other case, $[s^*-\bar{l}]_2 = [0]_2$, the circumscribed rectangle is quasi-standard.

The main property of the path ω^* is the following proposition.

Proposition 10. If $U_2 < U_1 < 2U_2 - 2\varepsilon$, $\varepsilon = U_1 + U_2 - \Delta$ is sufficiently small and L large enough, we have that

$$\{\arg\max_{\omega^*} H\} = \omega^* \cap \mathcal{P}. \tag{3.52}$$

Proof. Let us consider the skeleton path $\{\bar{\omega}_s\}_{s=0,\dots,2(L+2)}$, and let $\omega^*(\bar{\omega}_s, \bar{\omega}_{s+1})$ be the part of ω^* between $\bar{\omega}_s$ and $\bar{\omega}_{s+1}$, i.e., the interpolation of one step of the skeleton path.

Defining

$$g(s) := \max_{\eta \in \omega^*(\bar{\omega}_s, \bar{\omega}_{s+1})} H(\eta) \tag{3.53}$$

we have:

$$\max_{\eta \in \omega^*} H(\eta) = \max_{s=0,\dots,2(L+2)} g(s). \tag{3.54}$$

By the definition of ω^* we have that the function $g(s)$ takes the following values:

$$g(s) = \begin{cases} H(\bar{\omega}_s) + 2\Delta - U_1 & \text{if } s \leqslant 3\bar{l} \text{ and } [s]_3 \neq [0]_3, \text{ or } s > 3\bar{l}, \\ H(\bar{\omega}_s) - \varepsilon \frac{s}{3} + \Delta + U_1 & \text{if } s \leqslant 3\bar{l} \text{ and } [s]_3 = [0]_3. \end{cases} \tag{3.55}$$

Indeed for the values of s corresponding to steps a.1, a.2, and b.1 of the definition of the reference path, we can immediately verify that $g(s) = H(\bar{\omega}_s) + 2\Delta - U_1$. Steps a.3 and b.2 are more complicated since the reference path visits the quasi-domino and the quasi-standard configurations, respectively. In these cases we can easily verify the following:
if $s \leqslant 3\bar{l}$ and $[s]_3 = [0]_3$ then the path described in a.3 has a first part going from $\bar{\omega}_s$ to $\mathcal{R}^{\text{q-dom}}(s+1)$ reaching its maximal energy at $H(\bar{\omega}_s) + 2\Delta - U_1$. The second part of the path in a.3 goes from $\mathcal{R}^{\text{q-dom}}(s+1)$ to $\bar{\omega}_{s+1} \in \mathcal{R}^{\text{dom}}(s+1)$ with a maximal energy at $H(\mathcal{R}^{\text{q-dom}}(s+1)) + \Delta + U_1 - U_2 = H(\bar{\omega}_s) + U_2 - \varepsilon(s/3) + \Delta + U_1 - U_2$. We have:

$$\max\left\{H(\bar{\omega}_s) + 2\Delta - U_1,\ H(\bar{\omega}_s) - \varepsilon\frac{s}{3} + \Delta + U_1\right\} = H(\bar{\omega}_s) - \varepsilon\frac{s}{3} + \Delta + U_1. \tag{3.56}$$

In a similar way, for the standard regime, $s > 3\bar{l}$, if $[s - \bar{l}]_2 = [0]_2$ step b.2 gives:

$$\begin{aligned} &\max\left\{H(\bar{\omega}_s) + 2\Delta - U_1,\ H(\bar{\omega}_s) + U_2 - \varepsilon\frac{s-\bar{l}}{2} + \Delta + U_1 - U_2\right\} \\ &\quad = H(\bar{\omega}_s) + 2\Delta - U_1, \end{aligned} \tag{3.57}$$

which completes the proof of (3.55). ∎

We want now to evaluate the maximal value of $g(s)$ in the domino regime, i.e., for $s \leqslant 3\bar{l}$. The energy of domino configurations is an increasing function of s, for $s \leqslant 3\bar{l}$. More precisely the three functions:

$$\begin{aligned} h^{(0\text{-dom})}(n) &:= H(\mathcal{R}^{0\text{-dom}}(3n)) = (U_1 + 2U_2)n - 2\varepsilon n^2, \quad n = 0, \dots, \bar{l}, \\ h^{(1\text{-dom})}(n) &:= H(\mathcal{R}^{1\text{-dom}}(3n+1)) = U_1(n+1) + 2U_2 n \\ &\quad -2\varepsilon n(n+1), \quad n = 0, \dots, \bar{l} - 1, \\ h^{(2\text{-dom})}(n) &:= H(\mathcal{R}^{2\text{-dom}}(3n+2)) = U_1(n+1) \\ &\quad +U_2(2n+1 - \varepsilon(n+1)(2n+1), \quad n = 0, \dots, \bar{l} - 1 \end{aligned} \tag{3.58}$$

are increasing functions of n. This implies that:

$$\begin{aligned} \max_{s \leqslant 3\bar{l}} g(s) = \max\{&H(\bar{\omega}_{3\bar{l}-2}) + 2\Delta - U_1,\ H(\bar{\omega}_{3\bar{l}-1}) + 2\Delta - U_1, \\ &H(\bar{\omega}_{3\bar{l}}) + U_2 - \varepsilon\bar{l} + \Delta + U_1 - U_2\} \end{aligned}$$

and by a direct comparison we obtain immediately

$$\max_{s \leqslant 3\bar{l}} g(s) = H(\bar{\omega}_{3\bar{l}}) - \varepsilon\bar{l} + \Delta + U_1. \tag{3.59}$$

By Proposition 9 point (v), we have that in the standard regime, $s > 3\bar{l}$ the maximum value of $g(s)$ is obtained in s^*. To conclude the proof of the proposition we have to compare the maximal values of $g(s)$ in domino and standard regimes, since the energy of the configurations in T_3 can be made arbitrary small by choosing L large enough.

$$\begin{aligned} \max_{s=0,\dots,2(L+2)} g(s) &= \max\{\max_{s \leqslant 3\bar{l}} g(s), \max_{s=3\bar{l}+1,\dots,2(L+2)} g(s)\} \\ &= \max\{H(\bar{\omega}_{3\bar{l}}) - \varepsilon\bar{l} + \Delta + U_1,\ H(\bar{\omega}_{s^*}) + 2\Delta - U_1\} \\ &= H(\bar{\omega}_{s^*}) + 2\Delta - U_1. \end{aligned} \tag{3.60}$$

Indeed, if we define $\bar{\delta} \in (0, 1)$ by means of the equality $\bar{l} = ((U_1 - U_2)/\varepsilon) + 1 - \bar{\delta}$ we have immediately:

$$H(\omega_{3\bar{l}}) - \varepsilon\bar{l} + \Delta + U_1 = H(\omega_{3\bar{l}}) + 2\Delta - U_1 + \varepsilon\bar{\delta}. \tag{3.61}$$

On the other hand, by Proposition 9 (i) we have $s^* > 3\bar{l}$ so that $H(\omega_{s^*}) \geqslant H(\mathcal{R}^{\mathrm{st}}(3\bar{l}+1))$. By noting that $\omega_{3\bar{l}} \in \mathcal{R}^{\mathrm{st}}(3\bar{l})$ we have immediately that $U_1 < 2U_2 - 2\varepsilon$ implies:

$$H(\mathcal{R}^{\mathrm{st}}(3\bar{l}+1)) - H(\mathcal{R}^{\mathrm{st}}(3\bar{l})) = 2U_2 - U_1 - 2\varepsilon + 2\varepsilon\bar{\delta} > \varepsilon\bar{\delta} \tag{3.62}$$

so that

$$H(\omega_{s^*}) \geqslant H(\mathcal{R}^{\mathrm{st}}(3\bar{l}+1)) > H(\mathcal{R}^{\mathrm{st}}(3\bar{l})) + \varepsilon\bar{\delta} \tag{3.63}$$

and the proof of (3.60) is completed.

By the definition of ω^* it is immediate to show that the configurations where this maximum value of energy is obtained, are the configurations in $\omega^* \cap \mathcal{P}$. ∎

3.3. The Exit from the Set $\mathcal{B}$

We define:

$$\mathcal{B} := \left\{ \eta : \begin{array}{l} s(\eta) \leqslant s^*, \text{ or} \\ s(\eta) = s^*+1 \text{ and } v(\eta) \geqslant p_{\min}(\eta) - 1, \text{ or} \\ s(\eta) = s^*+2 \text{ and } v(\eta) \geqslant s^* + p_{\min}(\eta) - 2 \end{array} \right\}, \tag{3.64}$$

where s^* is defined in (1.44) and $p_{\min}(\eta) = p_1(\eta) \wedge p_2(\eta)$.

The main result of this section is given by the following proposition.

Proposition 11. For $H_{\min}(\partial\mathcal{B})$ as in (1.20), $(\partial\mathcal{B})_{\min}$ as in (1.21), Γ as in (1.46) and $\mathcal{P}$ as in (1.45), we have:

$$H_{\min}(\partial\mathcal{B}) = \Gamma \tag{3.65}$$

moreover

$$\text{if } (\bar{\eta}, \eta) \in (\partial\mathcal{B})_{\min} \quad \text{then } H(\bar{\eta}) \geqslant H(\eta) \quad \text{and} \quad \bar{\eta} \in \mathcal{P}. \tag{3.66}$$

In order to prove this proposition and in particular, in order to analyze the exiting move from $\mathcal{B}$, we prove a preliminary result on single moves.

Let $(\bar{\eta}, \eta)$ be a move, i.e., $P(\bar{\eta}, \eta) > 0$, we define

$$\Delta s := s(\eta) - s(\bar{\eta}). \tag{3.67}$$

We have the following lemma.

Lemma 12. Let $p_{\min}(\eta) \geqslant 4$, we have

(i) $|\Delta s| \leqslant 5$,

(ii) if $\Delta s = 1$ then $v(\eta) \geqslant p_{\min}(\eta) - 3$,
if $\Delta s = 2$ then $n(\bar{\eta}) \geqslant 1$ and $v(\eta) \geqslant 2p_{\min}(\eta) - 5$,
if $\Delta s = 3$ then $n(\bar{\eta}) \geqslant 2$ and $v(\eta) \geqslant 3p_{\min}(\eta) - 6$,
if $\Delta s = 4$ then $n(\bar{\eta}) \geqslant 3$ and $v(\eta) \geqslant 4p_{\min}(\eta) - 7$,
if $\Delta s = 5$ then $n(\bar{\eta}) \geqslant 4$ and $v(\eta) \geqslant 5p_{\min}(\eta) - 8$,

(iii) if $\Delta s = 1$ and $v(\eta) < p_{\min}(\eta) - 1$ then $n(\bar{\eta}) \geqslant 2$.

Proof of Lemma (12). We say that a line r (column or row in $\mathbb{Z}^2$) *becomes active* in the move from $\bar{\eta}$ to η if it was not active in $\bar{\eta}$ (i.e., $r \cap \bar{\eta}_{\text{cl}} = \emptyset$ see (1.10)) and it is active in η, $\eta_{\text{cl}} \cap r \neq \emptyset$. In a single move at most five lines can become active: these are the row and the column containing the new position of the moved particle, (we will call these lines r_1 and r_2, where r_1 is the line of the move, and r_2 is the line orthogonal to it), and the three lines through the three nearest–neighbor sites x_3, x_4, and x_5 of the particle after the move, excluding the site that it occupied in $\bar{\eta}$ (lines r_3, r_4, and r_5) (see Fig. 8).

Lines r_3, r_4, and r_5 become active only if in the corresponding sites x_3, x_4, and x_5, there was a free particle in $\bar{\eta}$, and the line r_1, corresponding to the move, becomes active only if the moving particle was free before the move, otherwise it was already present in $\bar{\eta}$. Each line of types 3, 4, and 5 becoming active, brings in the new configuration at least $p_{\min}(\eta) - 1$ vacancies; indeed $|r_i \cap \eta_{\text{cl}}| = 1$ for $i = 3, 4, 5$ since $r_i \cap \bar{\eta}_{\text{cl}} = \emptyset$; the line r_1 brings at least $p_{\min}(\eta) - 2$ vacancies, and the line r_2 brings at least $p_{\min}(\eta) - 3$ vacancies. Points (i) and (ii) immediately follow from this.

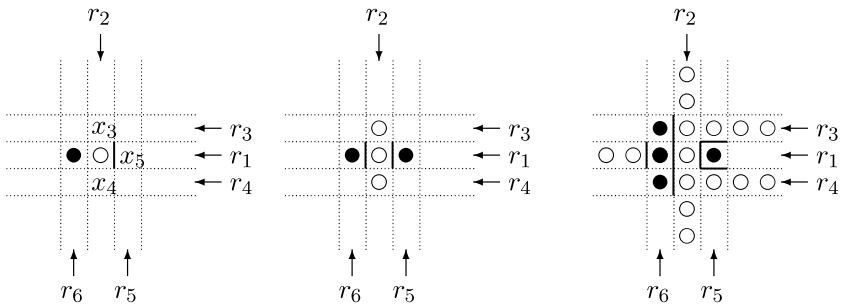

Figs. 8–10.

To prove (iii) suppose first that $\Delta s = 1$ with $k \geqslant 2$ activated lines and $k-1$ deactivated lines (i.e., lines which were active in $\bar{\eta}$ and that are not active in η). Since $k \geqslant 2$ activated lines bring at least $2p_{\min}(\eta) - 5$ vacancies, and $p_{\min}(\eta) \geqslant 4$ in this case $v(\eta) \geqslant 2p_{\min}(\eta) - 5 \geqslant p_{\min}(\eta) - 1$. So the only possibility to have $\Delta s = 1$ and $v(\eta) < p_{\min}(\eta) - 1$ is when there is only one line activated by the move and no deactivated lines, and this activated line is r_1 or r_2. If the activated line is r_1 and if it brings only $p_{\min}(\eta) - 2$ vacancies this means that in this line, in $\bar{\eta}$ there are two free particles, one of which is the moving particle. If the activated line is r_2, it brings $p_{\min}(\eta) - 3$ vacancies only if it contains 2 free particle before the move in the sites x_3 and x_4 (see Fig. 8); it bring $p_{\min}(\eta) - 2$ vacancies if it contain a free particle in sites x_3 or x_4 before the move. If the moving particle is free in $\bar{\eta}$, we have $n(\bar{\eta}) \geqslant 2$, if the moving particle is not free in $\bar{\eta}$, then line r_6 (see Fig. 8) was active in $\bar{\eta}$ and it is continue to be active in η. Due to the fact that r_2 is the unique line that become active, the line orthogonal to r_2 through this free particle (i.e., lines 3 or 4, say r_3 for concreteness) must be active in $\bar{\eta}$ and remains active in η. So we can conclude that there is an additional vacancy in η in the site $r_6 \cap r_3$, this implies that in this case $v(\eta) \geqslant p_{\min} - 2 + 1$.

Point (iii) is thus proved. ∎

Remark 13. We note that if $n(\bar{\eta}) = 0$ the unique line that can become active is r_2 and in this case in $\bar{\eta}$ sites x_3 and x_4 are empty and $x_5 \in \bar{\eta}_{\text{cl}}$, where $x_5 \in r_1$ (see Figs. 8 and 9), so that $\bar{\eta}$ is not monotonic $(g_1'(\bar{\eta}) + g_2'(\bar{\eta}) \geqslant 1)$ in this case.

Proof of the main proposition 11. Let $(\bar{\eta}, \eta) \in \partial\mathcal{B}$ be the exiting move from $\mathcal{B}$ and Δs be its corresponding variation of s. If $p_{\min}(\eta) \leqslant 3$, for $\varepsilon \ll U_2$, from explicit computations it follows:

$$H(\eta) > \Gamma. \tag{3.68}$$

Suppose from now on $p_{\min}(\eta) \geqslant 4$.

By using Lemma 12, we can distinguish seven different cases corresponding to $\Delta s = -1, 0, 1, 2, 3, 4, 5$, since, by definition, the only possibility to leave $\mathcal{B}$ with $\Delta s < 0$ is with $s(\bar{\eta}) = s^* + 2$ and $\Delta s = -1$.

Case -1. We will prove that if $\Delta s = -1$ and $(\bar{\eta}, \eta) \in \partial\mathcal{B}$ then $H(\bar{\eta}) \vee H(\eta) > \Gamma$. Since $s(\bar{\eta}) = s^* + 2$ we have that $H(\bar{\eta}) \leqslant \Gamma$ only if $n(\bar{\eta}) = 0$,

$g_1'(\bar\eta)+g_2'(\bar\eta)=0$ and $p_{\min}(\bar\eta)>3$. Indeed, for $p_{\min}(\bar\eta)\geqslant 4$ we have:

$$\begin{aligned} H(\bar\eta) &\geqslant H(\mathcal{R}^{\mathrm{st}}(s^*+2))+\varepsilon(s^*+p_{\min}(\bar\eta)-2)\\ &= H(\mathcal{R}^{\mathrm{st}}(s^*))+[H(\mathcal{R}^{\mathrm{st}}(s^*+2)-H(\mathcal{R}^{\mathrm{st}}(s^*)]+\varepsilon(s^*+p_{\min}(\bar\eta)-2)\\ &= H(\mathcal{R}^{\mathrm{st}}(s^*))+U_1+U_2+\varepsilon(p_{\min}(\bar\eta)-3)\\ &\geqslant H(\mathcal{R}^{\mathrm{st}}(s^*))+U_1+U_2. \end{aligned} \tag{3.69}$$

So if we add at least U_2 coming from $g_1'(\bar\eta)+g_2'(\bar\eta)\geqslant 1$ or $n(\bar\eta)\geqslant 1$ we have $H(\bar\eta)\geqslant H(\mathcal{R}^{\mathrm{st}}(s^*))+U_1+2U_2>\Gamma$.

In the case $s(\bar\eta)=s^*+2$ with $n(\bar\eta)=0$ and $g_1'(\bar\eta)+g_2'(\bar\eta)=0$, it is impossible to leave $\mathcal{B}$. Indeed, by Remark 13 it is impossible to activate lines and so $\Delta s=-1$ is obtained by a unique line becoming inactive. So we have $\Delta v:=v(\eta)-v(\bar\eta)\geqslant -p_{\max}(\bar\eta)$. By using the obvious relation: $p_{max}(\bar\eta)=s^*+2-p_{\min}(\bar\eta)$ we obtain

$$v(\eta)\geqslant s^*+p_{\min}(\bar\eta)-2-p_{max}(\bar\eta)=2p_{\min}(\bar\eta)-4\geqslant p_{\min}(\bar\eta)-1\geqslant p_{\min}(\eta)-1 \tag{3.70}$$

and so $\eta\in\mathcal{B}$ against $(\bar\eta,\eta)\in\partial\mathcal{B}$.

Case 0. This is the case of the minimal exit from $\mathcal{B}$. We have to distinguish two cases, indeed if $\Delta s=0$, then $(\bar\eta,\eta)\in\partial\mathcal{B}$ only if

(a) $s(\bar\eta)=s^*+1$ and $\Delta v\leqslant -1$,

(b) $s(\bar\eta)=s^*+2$ and $\Delta v\leqslant -1$.

Since the number of vacancies can decrease only if either $p_1(\eta)-p_1(\bar\eta)=p_2(\bar\eta)-p_2(\eta)\neq 0$ or $p_1(\eta)-p_1(\bar\eta)=p_2(\bar\eta)-p_2(\eta)=0$ but $|\eta_{\mathrm{cl}}|-|\bar\eta_{\mathrm{cl}}|>0$ that implies that in both case (a) and (b) we have:

(i) either $n(\bar\eta)\geqslant 1$ or

(ii) $n(\bar\eta)=0$ and, by Remark 13, $g_1'(\bar\eta)+g_2'(\bar\eta)\geqslant 1$ and r_2 become active bringing at least $p_{\min}(\eta)-1$ vacancies in η.

Case (a-i) contains the minimal exit from $\mathcal{B}$. Indeed by Proposition 8 we have $H(\bar\eta)\geqslant\Gamma$. Moreover if $\bar\eta\notin\mathcal{P}$ with $s(\bar\eta)=s^*+1$, $n(\bar\eta)\geqslant 1$ and $v(\eta)\geqslant p_{\min}-1$ we have that $H(\bar\eta)>\Gamma$ (see Proposition 8).
Case (a) is compatible only with case (i) because in case (a-ii) $v(\eta)\geqslant p_{\min}(\eta)-1$ and $s(\eta)=s(\bar\eta)=s^*+1$ implies $\eta\in\mathcal{B}$ against $(\bar\eta,\eta)\in\partial\mathcal{B}$. Cases (b-i) and (b-ii) can be treated as in point -1.

Case 1. Let $\Delta s = 1$, first suppose $s(\bar{\eta}) = s^*$; if $\eta \notin \mathcal{B}$ then $v(\eta) < p_{\min}(\eta) - 1$, indeed by Lemma 12, (iii) we have $n(\bar{\eta}) \geqslant 2$ and by Proposition 8 we can conclude

$$H(\bar{\eta}) \geqslant 2\Delta + H(\mathcal{R}^{\mathrm{st}}(s^*)) > \Gamma. \tag{3.71}$$

So we have only to consider the cases:

(a) $s(\bar{\eta}) = s^* + 1$,

(b) $s(\bar{\eta}) = s^* + 2$.

Again we consider two possibilities

(i) either $n(\bar{\eta}) \geqslant 1$ or

(ii) $n(\bar{\eta}) = 0$ and, by Remark 13, $g_1'(\bar{\eta}) + g_2'(\bar{\eta}) \geqslant 1$ and r_2 become active bringing at least $p_{\min}(\eta) - 1$ vacancies in η.

In case (a-i), by Proposition 8 we can conclude as in case (0.a-i)

In case (b-i) and (b-ii) we have immediately $H(\bar{\eta}) > \Gamma$ as obtained in point -1 (see (3.69))

We have only to discuss the case (a-ii). In this case the only line that can become active is r_2 and the configuration $\bar{\eta}_{\mathrm{cl}}$ is not connected. This also implies that there are no deactivating lines during the move. In this case we have to consider separately the case in which the move is horizontal or vertical.

(h) Suppose first that the move is horizontal, i.e., r_1 is an horizontal line (see Fig. 9). In this case we have $g_2'(\bar{\eta}) \geqslant 1$ and so by proposition 8, case b):

$$H(\bar{\eta}) \geqslant H(\mathcal{R}^{\mathrm{st}}(s^*)) + \Delta - U_1 + U_1. \tag{3.72}$$

Moreover if $g_2'(\bar{\eta}) \geqslant 2$ and/or $g_1'(\bar{\eta}) \geqslant 1$ we have immediately $H(\bar{\eta}) > \Gamma$. If $g_2' = 1$ and $g_1' = 0$, we have to consider the following cases:

– If the moving particle has in $\bar{\eta}$ at least one vertical and one horizontal bond connecting it to other particles, then $\Delta H \geqslant U_2$ and so $H(\eta) > \Gamma$.

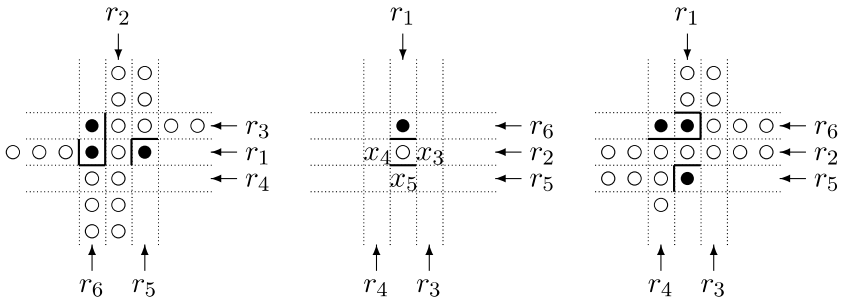

Figs. 11–13.

– If the moving particle has in $\bar{\eta}$ two vertical bonds connecting it to other particles (see Fig. 10), then $v(\bar{\eta}) \geqslant p_1(\bar{\eta}) + p_2(\bar{\eta}) - 2$ since, by the hypothesis $g_2'(\bar{\eta}) = 1$ $g_1'(\bar{\eta}) = 0$, in the lines r_1, r_3 we have over all at least $p_1(\bar{\eta}) - 1$ vacancies. As shown in (3.73) this implies $H(\bar{\eta}) > \Gamma$.

– If the moving particle has in $\bar{\eta}$ only one horizontal bond connecting it to other particles, then we can conclude that the line r_6 becomes inactive in the move, against $\Delta s = 1$.

– If the moving particle has in $\bar{\eta}$ only a vertical bond connecting it to other particles (see Fig. 11) as before, then we have $v(\bar{\eta}) \geqslant p_1(\bar{\eta}) + p_2(\bar{\eta}) - 2$. As shown in (3.73) this implies $H(\bar{\eta}) > \Gamma$.

The proof is completed in this horizontal case once we show that a configuration $\bar{\eta}$ with: $s(\bar{\eta}) = s^* + 1$, $n(\bar{\eta}) = 0$, $g_2'(\bar{\eta}) = 1$ and $v(\bar{\eta}) \geqslant p_1(\bar{\eta}) + p_2(\bar{\eta}) - 2$ has $H(\bar{\eta}) > \Gamma$. Indeed we have:

$$\begin{aligned} H(\bar{\eta}) &\geqslant H(\mathcal{R}^{\mathrm{st}}(s^* + 1)) + \varepsilon(s^* - 1) + U_1 \\ &> H(\mathcal{R}^{\mathrm{st}}(s^* + 1)) + \varepsilon(l_2^* - 1) + \Delta \geqslant \Gamma. \end{aligned} \tag{3.73}$$

(v) Suppose now that the move is vertical (see Fig. 12). In this case we have $g_1'(\bar{\eta}) \geqslant 1$ and so by Proposition 8

$$H(\bar{\eta}) \geqslant H(\mathcal{R}^{\mathrm{st}}(s^*)) + \Delta - U_1 + U_2. \tag{3.74}$$

We have to consider the following cases:

– If the moving particle has in $\bar{\eta}$ at least one vertical and one horizontal bond connecting it to other particles, then $\Delta H \geqslant U_1$ so that $H(\eta) > \Gamma$.

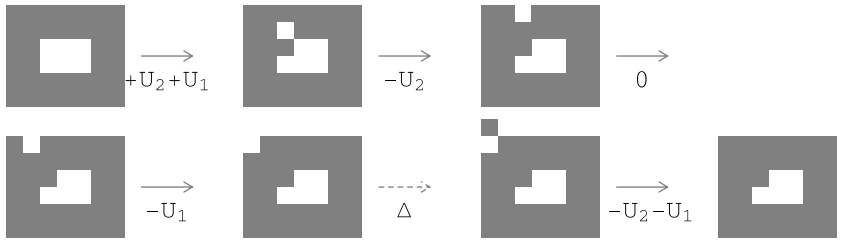

Fig. 14. (U_1+U_2)-reduction of a rectangle with a hole.

– If the moving particle has in $\bar{\eta}$ at least two horizontal bonds connecting it to other particles, then $\Delta H = -U_2 + 2U_1$ so that $H(\eta) > \Gamma$.

– If the moving particle has in $\bar{\eta}$ only one vertical bond connecting it to other particles, then we can conclude that the line r_6 becomes inactive in the move, against $\Delta s = 1$.

– If the moving particle has in $\bar{\eta}$ only one horizontal bond connecting it to other particles, then $\Delta H = U_1 - U_2$. If $g_1'(\bar{\eta}) = 1$ then $H(\eta) > \Gamma$ since $v(\bar{\eta}) \geqslant p_1(\bar{\eta}) + p_2(\bar{\eta}) - 2$ (see Fig. 13).

If $g_1'(\bar{\eta}) > 1$ then again we have $H(\eta) > \Gamma$.

The proof is completed in this vertical case if we prove that a configuration $\bar{\eta}$ with: $s(\bar{\eta}) = s^* + 1$, $n(\bar{\eta}) = 0$, $g_1'(\bar{\eta}) = 1$ and $v(\bar{\eta}) \geqslant p_1(\bar{\eta}) + p_2(\bar{\eta}) - 2$ has $H(\bar{\eta}) > \Gamma - U_1 + U_2$, that is $H(\eta) > \Gamma$. This computation is exactly the same as in the horizontal case (see Eq. (3.73))

Case 2. If $\Delta s = 2$, $(\bar{\eta}, \eta) \in \partial\mathcal{B}$ only if $s(\bar{\eta}) \geqslant s^*$, and by Lemma 12 we know that $n(\bar{\eta}) \geqslant 1$. If $s(\bar{\eta}) = s^* + 1$ and $n(\bar{\eta}) = 1$ we can conclude as in case (0.a-i). If $s(\bar{\eta}) = s^* + 2$ since $n(\bar{\eta}) \geqslant 1$ we have immediately $H(\bar{\eta}) > \Gamma$ (see Eq. (3.69)).

If $s(\bar{\eta}) = s^*$ and $n(\bar{\eta}) \geqslant 2$ then we have $H(\bar{\eta}) \geqslant 2\Delta + H(\mathcal{R}^{\mathrm{st}}(s^*)) > \Gamma$.

So we are left with the case: $s(\bar{\eta}) = s^*$ and $n(\bar{\eta}) = 1$.

If the unique free particle is the moving particle we can not have $\Delta s = 2$. Indeed r_3, r_4, and r_5 can not be activated and, in order to have $\Delta s = 2$, r_1 and r_2 have to become active. This implies that the sites x_3, x_4, and x_5 must be empty, but then $\Delta s = 0$.

If $g_1'(\bar{\eta}) + g_2'(\bar{\eta}) \geqslant 1$ we have

$$H(\bar{\eta}) \geqslant \Delta + H(\mathcal{R}^{\mathrm{st}}(s^*)) + U_2 > \Gamma \tag{3.75}$$

since $\Delta + U_2 > 2\Delta - U_1$. So we have to consider only the case $s(\bar{\eta}) = s^*$, $n(\bar{\eta}) = 1$, $g_1'(\bar{\eta}) = g_2'(\bar{\eta}) = 0$.

We distinguish two cases:

(a) the free particle is in site x_i, with i equal 3 or 4 the lines that become active are r_2 and r_i. Due to $g_1'(\bar{\eta}) = g_2'(\bar{\eta}) = 0$ the site x_5 is empty, and the site $\{x_3, x_4\} \backslash \{x_i\}$ is empty.

(b) the free particle is in site x_5 the lines that become active are r_2 and r_5 and the sites x_3 and x_4 are empty.

In both cases if the moving particle has in $\bar{\eta}$ at least one vertical and one horizontal bond connecting it to other particles, then $\Delta H \geqslant U_2$ and so $H(\eta) \geqslant H(\bar{\eta}) + U_2 \geqslant H(\mathcal{R}^{\mathrm{st}}(s^*)) + \Delta + U_2 > \Gamma$.

If the moving particle has in $\bar{\eta}$ either two bonds orthogonal to the move, or only one vertical or only one horizontal bond connecting it to other particles, then it is impossible to leave $\mathcal{B}$. Indeed in this case there exists a line r ($r = r_1$ or $r = r_6$) such that its intersection with $\bar{\eta}$ is only the moving particle. If $r = r_6$ then this line become inactive after the move against $\Delta s = 2$. If $r = r_1$ then the number of vacancies in η are at least the vacancies induced by the two activating lines and r_1. This means that in case (a) r_i and r_2 becomes active

$$|r_1 \cap \eta_{\mathrm{cl}}| = 1, \qquad |r_2 \cap \eta_{\mathrm{cl}}| = 2, \qquad |r_i \cap \eta_{\mathrm{cl}}| = 1 \tag{3.76}$$

so that

$$v(\eta) \geqslant p_1 - 1 + p_2 - 2 + p_{\min}(\eta) - 1 = s(\eta) + p_{\min}(\eta) - 4 = s^* + p_{\min}(\eta) - 2. \tag{3.77}$$

In case (b) lines r_5 and r_2 become active and

$$|r_1 \cap \eta_{\mathrm{cl}}| = 2, \qquad |r_2 \cap \eta_{\mathrm{cl}}| = 1, \qquad |r_5 \cap \eta_{\mathrm{cl}}| = 1 \tag{3.78}$$

so that

$$v(\eta) \geqslant p_1 - 2 + p_2 - 1 + p_{\min}(\eta) - 1 = s^* + p_{\min}(\eta) - 2 \tag{3.79}$$

and so $\eta \in \mathcal{B}$ against $(\bar{\eta}, \eta) \in \partial\mathcal{B}$.

Case 3. If $\Delta s = 3$, $(\bar{\eta}, \eta) \in \partial\mathcal{B}$ only if $s(\bar{\eta}) \geqslant s^* - 1$, and by Lemma 12 we know that $n(\bar{\eta}) \geqslant 2$. Therefore, we have

$$H(\bar{\eta}) \geqslant 2\Delta + H(\mathcal{R}^{\mathrm{st}}(s^* - 1)) > \Gamma \tag{3.80}$$

since $H(\mathcal{R}^{\mathrm{st}}(s^*+1)) - H(\mathcal{R}^{\mathrm{st}}(s^*-1)) = U_1 + U_2 - \varepsilon(s^*+1)$ and so $2\Delta + H(\mathcal{R}^{\mathrm{st}}(s^*-1)) = 2\Delta + H(\mathcal{R}^{\mathrm{st}}(s^*+1)) - U_1 - U_2 + \varepsilon(s^*+1) > H(\mathcal{R}^{\mathrm{st}}(s^*+1)) + \varepsilon(l_2^*-1) + \Delta = \Gamma$.

Case 4. If $\Delta s = 4$, $(\bar{\eta}, \eta) \in \partial\mathcal{B}$ only if $s(\bar{\eta}) \geqslant s^* - 2$, and by Lemma 12 we know that $n(\bar{\eta}) \geqslant 3$. Therefore, we have $H(\bar{\eta}) \geqslant 3\Delta + H(\mathcal{R}^{\mathrm{st}}(s^*-2)) > \Gamma$ as before.

Case 5. If $\Delta s = 5$, $(\bar{\eta}, \eta) \in \partial\mathcal{B}$ only if $s(\bar{\eta}) \geqslant s^* - 3$, and by Lemma 12 we know that $n(\bar{\eta}) \geqslant 4$. Therefore, we have $H(\bar{\eta}) \geqslant 4\Delta + H(\mathcal{R}^{\mathrm{st}}(s^*-3)) > \Gamma$ as before. ▌

3.4. Communication Height and Gate

By definition of communication height $\Phi(\underline{0}, \underline{1})$, by Proposition 10 we have immediately:

$$\Phi(\underline{0}, \underline{1}) \leqslant \max_i H(\omega_i^*) = H(\mathcal{P}) = \Gamma, \tag{3.81}$$

where $\mathcal{P}$ and Γ are defined in (1.45) and (1.46), respectively. On the other side, since every path going from $\underline{0}$ to $\underline{1}$ has to leave $\mathcal{B}$, we have by Proposition 11 that

$$\Phi(\underline{0}, \underline{1}) := \min_{\omega:\underline{0}\to\underline{1}} \max_{\zeta\in\omega} H(\zeta) \geqslant H_{\min}(\partial\mathcal{B}) = \Gamma. \tag{3.82}$$

By combining (3.81) and (3.82) we immediately obtain

$$\Phi(\underline{0}, \underline{1}) = \Gamma. \tag{3.83}$$

Note that to prove (3.83) we have applied the argument developed in ref. 11 with some small variations. In ref. 11, the set $\partial^+\mathcal{B}$ (external boundary of $\mathcal{B}$, see (1.17)) was considered, while here we use the set $\partial\mathcal{B}$ of exiting moves from $\mathcal{B}$ (see (1.19), so that in the present case $H_{\min}(\partial\mathcal{B})$ substitutes $H(\mathcal{F}(\partial^+\mathcal{B}))$.

The argument used to prove (3.83) also implies that $\mathcal{P}$ is a gate. Indeed given any optimal path ω, it has to leave $\mathcal{B}$ with a move in $(\partial\mathcal{B})_{\min}$ otherwise, by Proposition 11 we would have $\max_i H(\omega_i) > \Gamma$. To conclude we use (3.66).

3.5. Reduction

In this section we first prove the following proposition.

Proposition 14. There exists $\Gamma_0 < \Gamma$ such that $\mathcal{X}_{\Gamma_0} \subseteq \{\underline{0}, \underline{1}\}$, i.e.:

$$\forall \eta \neq \underline{0}, \underline{1} \quad \exists \eta' \in \mathcal{X} \quad \text{and a path } \omega : \eta \to \eta' \quad \text{s.t.}$$
$$H(\eta') < H(\eta), \quad \max_{\zeta \in \omega} H(\zeta) \leqslant H(\eta) + \Gamma_0. \tag{3.84}$$

In the second part of this section, as a corollary of this proposition, we will identify the stable and metastable states.

Proposition 15. If the side L of the box Λ is large enough ($L > 2l_1^*$ is a possible choice), then $V_{\underline{0}} = \Phi(\underline{0}, \underline{1})$ and $\underline{1} = \mathcal{X}^s$, $\underline{0} = \mathcal{X}^m$.

3.5.1. Reduction Outside $\{\underline{0}, \underline{1}\}$

To prove Proposition 14 we first characterize the set $\mathcal{X}_{U_1+U_2}$ of configurations which are not (U_1+U_2)-reducible, as follows.

Proposition 16. Any configuration $\eta \in \mathcal{X}_{U_1+U_2}$ has no free particles and it has only rectangular clusters with minimal side larger than 1.

We introduce some geometrical definitions. Let $\eta \in \mathcal{X}$ be given.

(i) A site $x \in \Lambda$ is connected trough empty (full) sites to $\partial^- \Lambda$ if there exists $x_1, \ldots, x_n$ a connected chain of nearest–neighbor empty (full) sites namely, $x_1 \in nn(x)$, $x_2 \in nn(x_1), \ldots,$ $x_n \in nn(x_{n-1})$, $x_n \in \partial^- \Lambda$ and $\eta(x_1) = \eta(x_2) = \cdots = \eta(x_n) = 0$ ($\eta(x_1) = \eta(x_2) = \cdots = \eta(x_n) = 1$).

(ii) An external corner of a set $A \subset \Lambda$ is a site $x \notin A$ such that $\sum_{y \in nn(x):(x,y) \in \Lambda^*_{0,h}} \chi_A(y) = 1$ and $\sum_{y \in nn(x):(x,y) \in \Lambda^*_{0,v}} \chi_A(y) = 1$, where χ_A is the characteristic function of the set A.

(iii) An internal corner of a set $A \subset \Lambda$ is a site $x \in A$ such that $\sum_{y \in nn(x):(x,y) \in \Lambda^*_{0,h}} \chi_A(y) = 1$ and $\sum_{y \in nn(x):(x,y) \in \Lambda^*_{0,v}} \chi_A(y) = 1$.

(iv) Let η^{ext} be the set of sites $x \in \Lambda_0$ such that $\eta(x) = 1$ and x is connected trough empty sites with $\partial^- \Lambda$.

Proof of Proposition 16. If η has a free particle then η is obviously 0-reducible, i.e., $\eta \notin \mathcal{X}_{U_1+U_2}$. The reducing path ω satisfying (3.84) is immediately obtained by bringing the free particle outside Λ or attaching it to a cluster.

Thus for each $\eta \in \mathcal{X}_{U_1+U_2}$ we have $\eta = \eta_{\text{cl}}$. Let $C_1(\eta), \ldots, C_n(\eta)$ be the clusters of η and let $\bar{C}_1(\eta), \ldots, \bar{C}_m(\eta)$ be the minimal simply connected sets of $\mathbb{R}^2$ containing $C_1(\eta), \ldots, C_n(\eta)$, i.e., the clusters whose holes have been filled up. We next show the following:

a. the sets $\bar{C}_i$ are rectangles with minimal side larger than one,

b. there are no holes inside the clusters: $C_i(\eta) = \bar{C}_i(\eta)$ for any i.

a. By definition the Euclidean distance between two different clusters in $\mathbb{R}^2$ is at least one. This implies that if there is a set $\bar{C}_i(\eta)$, which is not a rectangle, then there is an external corner x of η connected trough empty sites $x_1, \ldots, x_n$ to $\partial^- \Lambda$. This implies that η can be Δ-reduced. Indeed the reducing path, i.e., the path $\omega : \eta \to \eta'$ with $H(\eta') < H(\eta)$ and such that $\max_{\zeta \in \omega} H(\zeta) \leqslant H(\eta) + \Delta$, is given by the sequence of configurations ω_i with the same clusters as η plus a free particle that moves along the sequence $x_n, \ldots, x_1$, ($x_n \in \partial^- \Lambda$, x_1, a nearest–neighbor of the external corner x). In the final configuration ω_{n+1} the free particle is attached to the cluster in the site x. We have $H(\omega_i) \leqslant H(\eta) + \Delta$ for $i = 1, \ldots, n$ and $H(\omega_{n+1}) \leqslant H(\eta) + \Delta - (U_1 + U_2) < H(\eta)$.

If a set $\bar{C}_i(\eta)$ is made by a unique row (or a unique column) then the configuration η is obviously U_1-reducible (U_2-reducible) by removing a particle of the row (column) and bringing it out of Λ.

b. If one of the clusters of η has a hole, i.e., if there exists $C_i(\eta)$, which is not simply connected, then η can be $(U_1 + U_2)$-reduced (see Fig. 14).

Indeed, if such a cluster $C_i(\eta)$ exists, there exists also a cluster $C_{i_0}(\eta)$, possibly equal to $C_i(\eta)$, with holes and with $C_{i_0}(\eta) \cap \eta^{ext} \neq \emptyset$.

Let y be an internal corner of a hole of $C_{i_0}(\eta)$, connected to an internal corner y_n of $C_{i_0}(\eta)$ through full sites $y_1, y_2, \ldots, y_n$ and such that $y_n \in \eta^{ext}$. Such corners y and y_n exist since every set has at least four internal corners and since $C_{i_0}(\eta) \cap \eta^{\text{ext}} \neq \emptyset$.

Let $\eta_1, \eta_2, \ldots, \eta_n$ be the configurations obtained by moving the empty site from y to y_n through $y_1, \ldots, y_{n-1}$.

For any $i = 1, \ldots, n-1$, by using that y has at least 2 n.n. non-opposite occupied sites and that y_n has 2 n.n. non-opposite empty sites we have:

$$H(\eta_i) - H(\eta) \leqslant U_1 + U_2 \qquad \text{and} \qquad H(\eta_n) \leqslant H(\eta). \tag{3.85}$$

Moreover, by definition, y_n is an external corner of η_n, connected through empty sites to $\partial^- \Lambda$, so that η_n can be Δ-reduced as in point a. By joining the path $\eta_1, \eta_2, \ldots, \eta_n$ with the path realizing the Δ-reduction of η_n we obtain the $U_1 + U_2$-reduction of η.

Proof of Proposition 14. Suppose that $\eta \in \mathcal{X}_{U_1+U_2}$ and $\eta \neq \underline{0}, \underline{1}$, from Proposition 16 η has only rectangular clusters which are connected through empty sites to $\partial^- \Lambda$, i.e., $\eta^{\text{ext}} = \partial^- \eta$.

Suppose now that a rectangular cluster of η has a vertical subcritical side, i.e., $l_2 < l_2^*$, then it is possible to reduce η with the path described in Fig. 2 that removes a column of length l_2 with energy barrier $\Delta H(\text{remove column}) = U_1 + U_2 + \varepsilon(l_2 - 2) < 2\Delta - U_1$.

Otherwise if any rectangle in η has vertical supercritical sides, $l_2 \geqslant l_2^*$, it is possible to reduce η with the path described in Fig. 2 that adds a column with energy barrier $\Delta H(\text{add column}) = 2\Delta - U_1$.

The proof is complete by defining $\Gamma_0 := 2\Delta - U_1 < \Gamma$.

3.5.2. Stable and Metastable States

Proof of Proposition 15. Since $\mathcal{X}^{\text{s}} \subseteq \mathcal{X}_V$ for any $V \geqslant 0$ and since, if the side L of the volume Λ is large enough, we have $H(\underline{0}) > H(\underline{1})$, using also that by Proposition 14 we have $\mathcal{X}_{\Gamma_0} \subseteq \{\underline{0}, \underline{1}\}$, we can immediately conclude that $\mathcal{X}^{\text{s}} = \underline{1}$. If we are able to prove that

$$V_{\underline{0}} = \Phi(\underline{0}, \underline{1}) = \Gamma > \Gamma_0 \tag{3.86}$$

we can immediately conclude that $\underline{0} \in \mathcal{X}^{\text{m}}$.

Let us now prove (3.86). By definition we have that $V_{\underline{0}} \leqslant \Phi(\underline{0}, \underline{1})$. We argue by contradiction: suppose that $V_{\underline{0}} < \Phi(\underline{0}, \underline{1})$. Then, by definition, there exists $\eta^{(1)}$ with $H(\eta^{(1)}) < H(\underline{0})$ and $\Phi(\underline{0}, \eta^{(1)}) = V_{\underline{0}} < \Phi(\underline{0}, \underline{1})$. This implies that $\eta^{(1)}$ can not be equal to $\underline{1}$, so since by $\mathcal{X}_{\Gamma_0} \subseteq \{\underline{0}, \underline{1}\}$, we know that $\eta^{(1)} \notin \mathcal{X}_{\Gamma_0}$ we can iterate this argument by obtaining a sequence $H(\underline{0}) > H(\eta^{(1)}) > H(\eta^{(2)}) > \cdots > H(\eta^{(n)})$ with $\Phi(\eta^{(i)}, \eta^{(i+1)}) \leqslant H(\eta^{(i)}) + \Gamma_0 < \Phi(\underline{0}, \underline{1})$ if $\eta^{(i)} \neq \underline{1}$. The number of these iterations must be finite since the sequence $\eta^{(i)}$ has a strictly decreasing energy and the state space is finite. Moreover, the sequence stops at $\eta^{(n)} \in \mathcal{X}_{\Gamma_0}$ and we have $\eta^{(n)} = \underline{1}$ since $\mathcal{X}_{\Gamma_0} \subseteq \{\underline{0}, \underline{1}\}$ and $H(\eta^{(0)}) > H(\eta^{(n)})$. We obtain

$$\begin{aligned} \Phi(\underline{0}, \underline{1}) = \Phi(\underline{0}, \eta^{(n)}) &\leqslant \max\{\Phi(\underline{0}, \eta^{(1)}), \Phi(\eta^{(1)}, \eta^{(2)}), \ldots, \Phi(\eta^{(n-1)}, \eta^{(n)})\} \\ &< \Phi(\underline{0}, \underline{1}), \end{aligned} \tag{3.87}$$

which is absurde.

3.6. Proof of Theorem 3

To prove Theorem 3 we need the notion of cycle that is one of the main tools used in the general theory of Freidlin–Wentzell Markov chains. We shortly recall the definition in our case.

A *non-trivial cycle* is a connected set $\mathcal{C} \subset \mathcal{X}$ such that

$$\max_{\sigma \in \mathcal{C}} H(\sigma) < H(\mathcal{F}(\partial^+ \mathcal{C})). \tag{3.88}$$

Any singleton that is not a non-trivial cycle is called *trivial cycle*.

The following result represents the main property of cycles (see for instance refs. 11 and 15 Theorem 2.17): with large probability every state in a cycle is visited by the process before the exit.

Proposition 17. Let $\mathcal{C}$ be a cycle. There exists $K > 0$ such that for any $\eta, \eta' \in \mathcal{C}$ and for all sufficiently large β

$$\mathbb{P}_\eta(\tau_{\eta'} < \tau_{\partial^+ \mathcal{C}}) \geqslant 1 - e^{-K\beta}. \tag{3.89}$$

By using this resut, to prove Theorem 3 it is sufficient to show the following:

(i) if η is a rectangular configuration contained in $\mathcal{R}(l_1^* - 1, l_2^* - 1)$, then there exists a cycle $\mathcal{C}_{\underline{0}}$ containing η and $\underline{0}$ and not containing $\underline{1}$;

(ii) if η is a rectangular configuration containing $R \in \mathcal{R}(l_1^*, l_2^*)$, then there exists a cycle $\mathcal{C}_{\underline{1}}$ containing η and $\underline{1}$ and not containing $\underline{0}$.

We start by showing (i). Let $\mathcal{C}_{\underline{0}}$ be the maximal connected set containing $\underline{0}$ such that $\max_{\eta' \in \mathcal{C}_{\underline{0}}} H(\eta') < \Gamma$. By definition $\mathcal{C}_{\underline{0}}$ is a cycle containing $\underline{0}$. It does not contain $\underline{1}$ since $\Phi(\underline{0}, \underline{1}) = \Gamma$. We have only to prove that $\mathcal{C}_{\underline{0}}$ contains η. This can be easily obtained by constructing a path $\omega^{\eta, \underline{0}}$ going from η to $\underline{0}$ keeping the energy less than Γ. $\omega^{\eta, \underline{0}}$ is obtained by erasing site by site, each column of η and by showing that all the configurations of this path are in $\mathcal{C}_{\underline{0}}$.

More precisely, let $\eta = \{(x, y) \in \mathbb{Z}^2; \quad x \in (n, n + l_1],\ y \in (m, m + l_2]\} \in \mathcal{R}(l_1, l_2)$ for some $n, m \in \mathbb{Z}$, and let $\{\bar{\omega}_i^{\eta, \underline{0}}\}_{i=0,\ldots,l_1}$ be a path of rectangular configurations, starting from η and ending in $\underline{0}$, given by

$$\bar{\omega}_i^{\eta, \underline{0}} = \{(x, y) :\ x \in (n, n + l_1 - i],\ y \in (m, m + l_2]\}. \tag{3.90}$$

To complete the construction we can use now the same idea applied in the definition of the reference path ω^*: between every pair $\bar\omega_i^{\eta,\underline{0}}, \bar\omega_{i+1}^{\eta,\underline{0}}$ we can insert a sequence $\tilde\omega_{i,0}^{\eta,\underline{0}}, \dots, \tilde\omega_{i,l_2}^{\eta,\underline{0}}$, where $\tilde\omega_{i,0}^{\eta,\underline{0}} = \bar\omega_i^{\eta,\underline{0}}$ and for $j > 0$, $\tilde\omega_{i,j}^{\eta,\underline{0}}$ is obtained by $\bar\omega_i^{\eta,\underline{0}}$ by erasing j sites:

$$\tilde\omega_{i,j}^{\eta,\underline{0}} = \bar\omega_i^{\eta,\underline{0}} \setminus \{(x, y):\ x = n + l_1 - i,\ y \in [m + l_2 - j, m + l_2]\}. \tag{3.91}$$

Again, as in the reference path ω^*, the last interpolation consists in inserting between every pair of consecutive configurations in $\tilde\omega^{\eta,\underline{0}}$ a sequence of configurations with a free particle in a suitable sequence of sites going from the site previously occupied by the erased particle to $\partial\Lambda$. Since for any $l_1 \leqslant l_1^* - 1$ and $l_2 \leqslant l_2^* - 1$ we have $H(\mathcal{R}(l_1, l_2)) < H(\mathcal{R}(l_1^* - 1, l_2^*))$, for the path $\omega^{\eta,\underline{0}}$ obtained in this way we have:

$$\max_i H(\omega_i^{\eta,\underline{0}}) = \max_{l \in [1, l_1 - 1]} H(\mathcal{R}(l, l_2)) + 2\Delta - U_1 < \Gamma. \tag{3.92}$$

The proof of (ii) is similar. Let $\mathcal{C}_{\underline{1}}$ be the maximal connected set containing $\underline{1}$ such that $\max_{\eta' \in \mathcal{C}_{\underline{1}}} H(\eta') < \Gamma$. Again $\mathcal{C}_{\underline{1}}$ is by definition a cycle containing $\underline{1}$ and not containing $\underline{0}$ since $\Phi(\underline{0}, \underline{1}) = \Gamma$. To prove that $\mathcal{C}_{\underline{1}}$ contains η we define now a path $\omega^{\eta,\underline{1}}$ going from η to $\underline{1}$ obtained by reaching first of all the standard shape and, from there, following the path ω^*. As before, it is easy to show that all the configurations of this path have an energy smaller than Γ so that they are in $\mathcal{C}_{\underline{0}}$.

Going into the details, let $\eta \in \mathcal{R}(l_1, l_2)$; let us suppose that $[l_1 + l_2 - \bar l]_2 = [0]_2$, since the other case, $[l_1 + l_2 - \bar l]_2 = [1]_2$, can be treated in a similar way. If $l_1 - l_2 = \bar l$ then η is standard and $\omega^{\eta,\underline{1}}$ can be chosen as the part of the reference path ω^* going from η to $\underline{1}$. If $l_1 - l_2 < \bar l$ then first add columns to η, with the mechanism similar to the time reversal of the one used in the construction of $\omega^{\eta,\underline{0}}$, until we reach the standard rectangle in $\mathcal{R}(l_2 + \bar l, l_2)$. The remaining part of the path follows ω^* from $\mathcal{R}(l_2 + \bar l, l_2)$ to $\underline{1}$. If $l_1 - l_2 > \bar l$ then first move columns to rows following the mechanism given in steps a.3 and b.2, until we reach a standard rectangle. From there, follow the reference path ω^*. For the path $\omega^{\eta,\underline{1}}$ obtained in this way, by using that in our parameter regime $\Delta + U_1 - U_2 < 2\Delta - U_1$, and that $H(\mathcal{R}(l_1', l_2')) < H(\mathcal{R}(l_1^* - 1, l_2^*))$, for any $l_1' \geqslant l_1^*$ and $l_2' \geqslant l_2^*$, we obtain:

$$\max_i H(\omega_i^{\eta,\underline{1}}) \leqslant \max_{l_1' \geqslant l_1^*, l_2' \geqslant l_2^*} H(\mathcal{R}(l_1', l_2')) + 2\Delta - U_1 < \Gamma \tag{3.93}$$

so that $\omega_i^{\eta,\underline{1}} \in \mathcal{C}_{\underline{1}}$ for any i and the proof of theorem 3 is complete. ∎

ACKNOWLEDGMENTS

The research in this paper was partially supported by MURST-grant Cofinanziamento 2000 Scienze Fisiche/21.

REFERENCES

1. G. B. Arous and R. Cerf, Metastability of the three-dimensional Ising model on a torus at very low temperature, Electron. *J. Probab*. 1 Research Paper **10** (1996).
2. D. Capocaccia, M. Cassandro, and E. Olivieri, A study of metastability in the Ising model, *Commun. Math. Phys.* **39**:185–205, (1974).
3. M. Cassandro, A. Galves, E. Olivieri, and M. E. Vares, Metastable behaviour of stochastic dynamics: A pathwise approach, *J. Statis. Phys.* **35**:603–634 (1984).
4. E. N. M. Cirillo and F. R. Nardi, Metastability for a stochastic dynamics with parallel heath bath updating rule, *J. Statist. Phys.* **110**:183–217 (2003).
5. E. N. M. Cirillo and E. Olivieri, Metastability and nucleation for the Blume–Capel model: Different mechanism of transition, *J. Statist. Phys.* **83**:473–554 (1996).
6. A. Gaudilliére, E. Olivieri, and E. Scoppola, Nucleation pattern at low temperature for local Kawasaki dynamics in two dimensions, Preprint.
7. F. den Hollander, F. R. Nardi, E. Olivieri, and E. Scoppola, Droplet growth for three-dimensional Kawasaki dynamics, *Prob. Theory Relat. Fields* **125**:153–194 (2003).
8. F. den Hollander, E. Olivieri, and E. Scoppola, Metastability and nucleation for conservative dynamics, *J. Math. Phys.* **41**:1424–1498 (2000).
9. R. Kotecký, and E. Olivieri, Droplet dynamics for asymmetric Ising model, *J. Statist. Phys*. **70**:1121–1148 (1993).
10. R. Kotecký and E. Olivieri, Shape of growing droplets-A model of escape from a metastable phase, *J. Statist. Phys*. **75**:409–507 (1994).
11. F. Manzo, F. R. Nardi, E. Olivieri, and E. Scoppola, On the essential features of metastability: tunnelling time and critical configurations, *J. Statist. Phys.* **115**:591–642 (2004).
12. F. R. Nardi and E. Olivieri, Low temperature stochastic dynamics for an Ising model with alternating field, *Markov Process. Relat. Fields* **2**:117–166 (1996).
13. E. Olivieri and E. Scoppola, Markov chains with exponentially small transition probabilities: First exit problem from a general domain. I. The reversible case, *J. Statis. Phys.* **79**:613–647 (1995).
14. E. Olivieri and E. Scoppola, Markov chains with exponentially small transition probabilities: First exit problem from a general domain. II. The general case, *J. Statis. Phys*. **84**:987–1041 (1996).
15. E. Olivieri and M. E. Vares, *Large Deviations and Metastability* (Cambridge University Press, 2005).